의학박사 학위논문

Functional study of recombinant *Clonorchis sinensis* thioredoxin peroxidase on inhibitory effect of macrophage activation

재조합한 간흡충 thioredoxin peroxidase 의 대식세포 기능 억제 효능 연구

2014 년 8 월

서울대학교 대학원

의학과 기생충학전공

위 해 주

A thesis of the Degree of Doctor of Philosophy

재조합한 간흡충 thioredoxin peroxidase 의 대식세포 기능 억제 효능 연구

Functional study of recombinant *Clonorchis sinensis* thioredoxin peroxidase on inhibitory effect of macrophage activation

August 2014

The Department of Medicine,

Seoul National University

College of Medicine

Hae Joo Wi

Functional study of recombinant *Clonorchis sinensis* thioredoxin peroxidase on inhibitory effect of macrophage activation

by
Hae Joo Wi
(Directed by Prof. Young Mee Bae)

A thesis submitted to the Department of Medicine in partial fulfillment of the requirements for the Degree of Doctor of Philosophy in Medicine (Parasitology and Tropical Medicine) at Seoul National University College of Medicine

August 2014
Approved by Thesis Committee:

Professor _____Chairman
Professor _____Vice chairman
Professor _____
Professor _____
Professor _____

재조합한 간흡충 thioredoxin peroxidase 의 대식세포 기능 억제 효능 연구

지도 교수 배 영 미

이 논문을 의학박사 학위논문으로 제출함
2014년 8월

서울대학교 대학원
의학과 기생충학 전공
위 해 주

위해주의 의학박사 학위논문을 인준함
2014년 8월

위 원 장 _____ (인)
부위원장 _____ (인)
위 원 _____ (인)
위 원 _____ (인)
위 원 _____ (인)

ABSTRACT

Clonorchis sinensis (*C. sinensis*) estabilishes long term parasitism within bile ducts of humans without notable symptoms. General down-modulated host immune responses in helminth infestation are maintained by excretory-secretory products (ESP), produced by the live parasites and considered as an important immunomodulator in this context. Co-culture experiments with RAW264.7 cells and *C. sinensis* adults worms through permeable transwell demonstrated that ESP from living *C. sinensis* functioned as a ligand for TLR4, but effectively attenuated LPS-induced IL-6 and NO production. On the other hands, upsurged secretion of anti-inflammatory cytokines IL-10 and TGF-β were observed by *C. sinensis* ESP treatment. Reference base study found out that thioredoxin peroxidase (TPX) of helminth parasites had an immune-modulating property toward Th2 type through induction of regulatory phenotype of macrophages. Hence, recombinant TPX of *C. sinensis* was produced and its gene was registered at Genbank (AND65138.1). The CS-TPX reduced LPS-induced expression of TLR4 on cell surface of RAW264.7 cells and LPS-induced secretion of pro-inflammatory mediators NO, TNF-α and IL-6. Moreover, CS-TPX induces IL-10, but not TGF-β. Pull-down assay result revealed the direct interaction between CS-TPX and TLR4 protein. Furthermore, the smallest recombinant fragment of CS-TPX, which is T44, has comparable anti-inflammatory. In conclusion, this study described the macrophage regulatory function of *C. sinensis* ESP and the smallest fragment of CS-TPX, T44, could function of the negative regulator in LPS treated macrophage cell line RAW264.7 cells. Defined CS-TPX T44 will be one of the best candidates for therapeutic immunosuppressant in allergies and

autoimmune diseases.

Keywords: *Clonorchis sinensis*, thioredoxin peroxidase, deletional mutant, site-directed mutagenesis, immune evasion, LPS, IL-10, TGF-β, nitric oxide, IL-6, macrophages

Student number: 2010-31160

CONTENTS

LIST OF FIGURES

LIST OF TABLES

LIST OF ABBREVIATIONS

C. sinensis	*Clonorchis sinensis*
TPX	Thioredoxin peroxidase
mTPX	Mutant TPX
ESP	Excretory-secretory products
CA	Crude antigen of *C. sinensis*
EA	Egg antigen of *C. sinensis*
LPS	Lipopolysaccharide
NO	Nitric oxide
IL	Interleukin
TNF-α	Tumor necrosis factor-alpha
TGF-β	Transforming growth factor-beta
TLR	Toll-like receptor
NF-κB	Nuclear factor kappa-light-chain-enhancer of activated B cells
MAPK	Mitogen-activated protein kinase
SE	Standard error

INTRODUCTION

Clonorchis sinensis Looss, 1907 is a liver fluke that parasitizes in the biliary tract of humans, dogs, cats, pigs and minks. It is limitedly distributed in East Asia including Korea, China, Far East Russia, Taiwan as well as Vietnam and it is highly endemic in some regions (1). Endemicity of clonorchiasis is determined by the fish-eating customs among residents because metacercariae of *C. sinensis* existed in flesh of fishes. In Korea, the national survey for the status of intestinal helminthiasis in 2004 demonstrated that the egg positive rate of *C. sinensis* reached 2.9% and estimated 1.3 million people suffered from clonorchiasis (2). Therefore, clonorchiasis is one of the major public health problems in Korea.

Upon infestation with *C. sinensis,* most of the live metacercariae enter into bile ducts and fulfill a successful parasitic life cycle so that most of the infected humans show minor symptoms. General complications such as epigastric pain, diarrhea, fever and loss of appetite as well as jaundice are shown in only heavily infected subjects (3). Likewise, mild symptoms of infection make infected human to ignore medical examination and carry worms for more than 10 years (1). Major pathologic transformation of clonorchiasis had included with adenomatous hyperplasia of biliary epithelium, irregular ductal dilatation, periductal inflammation and fibrosis (1, 4-6). Moreover, considerable reports provided evidences that cholangiocarcinoma is induced by clonorchiasis not only in animal model but also in human so that the possible correlation was addressed (6-9). Thus, International Agency for Research on Cancer categorized the *C. sinensis* as a risk factor for hepatobiliary cancer (class I carcinogen group) in 2009.

Moreover, *C. sinensis* produce complex-metabolites, excretory-secretory products (ESP), and stimulate proliferation of HEK 293 cells as well as HuCCT-1 cells, which implied that ESP from *C. sinensis* had critical role for inducing cholangiocarcinoma (10, 11). Differential gene regulation of human cholangiocarcinoma cells upon *C. sinensis* ESP treatment revealed that 23,920 human genes were affected (12). Among them, activation of minichromosome maintenance protein 7 (Mcm7) along with histone acetyltransferase (HAT) expression was crucial for carcinogenesis upon *C. sinensis* ESP treatment (13). Since major health problem with clonorchiasis is cholangiocarcinoma, numerous investigations were focused on worm and carcinogenesis without immunological explanation.

It is well-known that suitable animal model of *C. sinensis* infection is Syrian golden hamster because it is susceptible to infestation and synergistically develop cholangiocarcinoma upon dimethylnitrosamin (DMN) treatment (14). However, limited diversity of commercial antibodies for hamsters makes it difficult to study in detailed mechanisms. Alternatively, mice would be the good research model for host-*C. sinensis* relationship study because of wide variety of commercial antibodies. Susceptibility to *C. sinensis* infection varies in each mouse strains examined (15, 16). Among them, FVB/NJ mice produce higher levels of serum IgE and IL-4 producing splenocytes in response to concanavalin-A (ConA) after *C. sinensis* infection than BALB/c mice (15). Not only a Th2 type immune responses but also haplotype of major histocompatibility (MHC) would be suspected factors that influence outcome of infectivity. However, CBA/N and C57BL/6 mice are incomplete model for infection because they discharge *C. sinensis* worm from their liver at 10 weeks after post-infection and do not develop cholangiocarcinoma (Yan Jin et al., unpublished data). Therefore, further

study to clarify immunological mechanisms which influences susceptibility is urgent and relationship between chronic infection and carcinogenesis has to be elucidated.

Chronic clonorchiasis in humans might be the critical factor for pathological transformation, such as ductal inflammation and cholangiocarcinoma. Therefore, it was curious that how *C. sinensis* establishes a long term parasitism within such a harmful environment without notable symptoms. Crispe I.N. explained that kupffer cells could acquire tolerogenic properties in response to lipopolysaccharide (LPS) such as the production of IL-10 and expression of PD-L1 co-inhibitory molecule. Furthermore, cross talk of kupffer cells with NK cells and T cells makes them unresponsiveness to toxin through portal vein (17).

General features of helminth infection represent attenuated Th2 type immune responses including hypo-responsiveness of T cells, anergic T cells, increased portion of regulatory T cells and high production of IL-10 and TGF-β (18-20). Not only T cells but also B cells went through such changes like increasing parasite-specific IgG, IgG4 antibody which helps regulatory T cell functions (21, 22). Dendritic cell (DC) is in charge of this attenuated Th2 immunity as one of the antigen presenting cells (APC). However, alternatively activated macrophages (AAM) in helminth infection play crucial role in both repairing tissue damage and suppressing T cell proliferation (23-26). Interestingly, reduced reactivities to allergens as well as auto-antigens were demonstrated in animal model of helminth infection (27) and in helminth infected humans (28, 29). What made down-modulated host immune responses in helminth infection is came from live parasites because chemotherapy for eradication of the parasites restored the responsiveness to antigens *in vivo* and *in vitro* (30, 31). Thus, ESPs originated from live

helminthes is considered as an important immunomodulator in its context (32, 33).

The ESPs are composed of metabolic by-products emitted from excretory/secretory organs and cuticle or tegument surfaces released from certain stage of parasite's body (32). And effects of ESPs on host immune regulations were well-known following species of parasites. *Fasciola hepatica* (*F. hepatica*) ESP treated DCs showed semi-mature phenotype upon LPS treatment and polarized $CD4^+$ T cells in to Th2 as well as Treg population (34). In cases of *Schistosoma mansoni* (*S. mansoni*), it is reported that ESP from skin penetrating larvae affect DC to drive Th2 type immune responses (35). Also, Omega-1 secreted from *S. mansoni* eggs activates DC so that it skews Th2 response through mannose receptor pathway (36). Interestingly, ESP of *Heligmosomoides polygyrus* (*H. polygyrus*) have a TGF-β-like function itself so that it trigger signaling through the TGF-β pathway which can induce de novo $Foxp3^+$ regulatory T cells (37). Not only the proteins but also glycan have the effective immunomodulating property and there are non-host-like as well as host-like glycan in helminth ESP. A number of host-mimicry glycans interact with C-type lectin receptors such as DC-SIGN, mannose receptor expressed on DC as well as macrophages and finally suppress immune responses (38-40). As remarked above, ESP has multi-functional mechanism for regulating host immune status to promote longer survival of worm itself. The systemic approaches to discover defined products which have immunoregulatory properties increase the possibilities for development of therapeutic molecules from helminth ESP. Table 1 described the representative defined products and main effect are summarized (Table 1).

Table 1. Immunomodulatory molecules originated from helminth parasites.

Products	Origin	Mode of action	Ref
ES-62	*A. vitae*	Anti-inflammatory (prevents collagen induced arthritis)	(41) (42)
		Protects against allergic airway hyperresponsiveness and skin hypersensitivity	
Omega-1	*S. mansoni*	Essential for induction of Th2 immune response	(43)
Lyso-PC	"	Stimulates IL-10 producing regulatory T-cells	(44)
LNFPIII	"	IL-10, PGE2 production Th2 type anti-inflammation	(45)
Cathepsin cysteine proteases	" / *F. hepatica*	Inhibit LPS-induced macrophage activation (inhibition of TRIF)	(46)
Cystatin	*O, volvulus*	Induces cell hypo-responsiveness	(47)
	/ A. vitae	Induces IL-10-producing macrophages	(48)
Calreticulin	*H. polygyrus*	Promote Th2 immunity	(49)
2-Cys peroxiredoxin	*F. hepatica*	Inducing AAM	(50)
		Initiate Th2 immunity	(51)

It is reasonable that *C. sinensis* worms could be attacked by reactive oxygen species (ROS) including hydroxyl radicals ($^{\bullet}OH$), superoxide anion ($O_2^{\bullet-}$) and hydrogen peroxide (H_2O_2) while they resides in the bile duct. The ROS are known to be produced by not only normal aerobic cellular metabolism but also host defense phagocytic cells. Especially, host innate immune cells such as eosinophils, neutrophils, macrophages recognize the invading pathogens and produce ROS to threaten or kill the pathogens even relatively large organism such as parasites (52, 53). Therefore, antioxidant system of the parasites might be necessary to overcome the oxidative stress as well as to protect from host immune reactions.

As mammalian cells have conserved series of antioxidant system (54), all helminth parasites developed their own antioxidant system (52, 53). Antioxidant defense against numerous oxidative stress can be managed by powerful antioxidant enzyme such as superoxide dismutase (SOD), catalase, glutathione peroxidase (GPX). Initially, SOD convert the free radical $O_2^{\bullet-}$ to H_2O_2 and then toxic product H_2O_2 can be neutralized by catalase or GPX reaction (55).

However, it was reported that of H_2O_2 catalysis enzymes lacked in a number of parasites. For instance, *S. mansoni* is deficient in catalase and has low activity of GPX (56). *Onchocerca volvulus* (*O. volvulus*) seems to be lacking in GPX (57) and the enzymatic activity of catalase and GPX appeared very limited in *O. cervicalis* (52). Alternatively, thioredoxin peroxidase (TPX) was identified and spotlighted as a major detoxifying factor for H_2O_2 in parasitic organisms such as *F. hepatica* (58), *S. mansoni* (59) and *Ascaris suum* (60).

TPX, also called 2-Cys peroxiredoxin, is a thiol-based peroxidase and was initially discovered as peroxide detoxifying enzymes in yeast (54, 61). It is

conserved in all kingdoms of organisms and the main function is to neutralize H_2O_2 and organic peroxides to water using peroxide reactivity of the cysteine sulfur atom and thioredoxin as the hydrogen-donor pathway (62).

In addition to their H_2O_2 scavenging actions, TPX is involved in various biological functions, such as apoptosis, cell proliferation, differentiation, intracellular signaling and immune regulation (63-66). Especially, endogenous deletion of TPX lead to enhanced proliferation of ConA-stimulated splenocytes and increased activity of DCs in mixed lymphocyte reaction (MLR) (66). Moreover, the essential role of TPX as negative regulator in LPS-induced macrophage activation and animal model for endotoxin-induced lethal shock was also investigated (67). Therefore, it suggested that TPX had an important function in the attenuation of elevated host immune responses.

Given that the regulatory effect of endogenous TPX, exogenous TPX from parasite to host seems to exert influence on surrounding cells and tissues. For example, recombinant TPX from *F. hepatica* directly modifies macrophages into Fizz1, Ym1, Arg1 expressing AAMs. And also high production levels of IL-10, prostaglandin E2 make it possible to estimate that the AAMs are regulatory phenotype (50). Interestingly, it is reported that macrophage differentiation into AAMs which activated by TPX is an essential step for the induction of Th2 immune responses by helminth parasite (51). Consistent with previous findings, it is presumed that the TPX from *C. sinensis* also be inherent in immune regulatory activities.

In this study, macrophage regulatory functions of *C. sinensis* ESP were unveiled and function of recombinant CS-TPX was described as one of the immune-regulatory protein among ESP. Since smallest CS-TPX-T44 has comparable inhibitory effect in LPS-induced RAW264.7 cells, it has important value for further investigation to develop a stable and effective immunosuppressant drug.

MATERIALS AND METHODS

1. Parasite collection, protein and RNA extraction

C. sinensis metacercariae were collected from naturally infected freshwater fish (*Pseudorasbora parva*) harvested at Shenyang City, Liaoning Province, People's Republic of China, which is an endemic site of clonorchiasis. With 0.6% pepsin–HCl solution as artificial gastric juice, fleshes of the fishes were digested in order to obtain the metacercariae. The metacercariae were then introduced into 5-week-old Sprague–Dawley rats. Two months after rats were infected with 50 metacercariae, adult *C. sinensis* worms were collected from the bile ducts and washed several times with phosphate-buffered saline (PBS) containing 150 μg/ml penicillin and 150 U/ml streptomycin. Finally, each worm was selected that has uniform size of length to use for co-culture with RAW264.7 cells.

For protein collection originated from *C. siensis*, isolated live adult worms were cultured in phenol-red free RPMI1640 medium (11835, Gibco, USA) containing antibiotics for 72 h under an atmosphere of 5% CO^2 at 37°C. After culture of the worms, the worm ESP containing medium was centrifuged for 30min at 13,200 rpm and then filtered with a 0.2-μm syringe filter. Filtered soluble protein regarded as ESP and pellet regarded as egg of worms. The whole worms and eggs antigen (EA) were homogenized in PBS containing antibiotics, separately. PBS-soluble crude antigens of the worms (CA) and EA were collected after centrifugation at 13,200 rpm for 10min at 4°C and then filtered with a 0.2-μm syringe filter. The protein concentration in the extract was measured using a BCA protein assay kit (Pierce, USA). Total RNA of the adults worm was extract using RNeasy protect mini kit (74126, Qiagen,

Germany) according to the manufacturer's instruction and stored at -70℃ until use.

2. Cell culture and worm co-culture

Murine macrophage RAW 264.7 cells were cultured in complete DMEM (Gibco) containing 10% FBS, 100μg/ml penicillin, 100 U/ml streptomycin at 37°C under humidified atmosphere of 5% CO_2. The cells with 8×10^4 cells/well were cultured within 24-well culture plates for 72 h with or without 10ng/ml LPS for co-culture study. Inserts type of transwell which had 6.5 mm diameter (Transwell®, 3422, Corning, USA) and 8.0 μm permeable pore size were used to separate cells and worms. Within transwell, 100 μl of culture media were added and then indicated number of worms were loaded (indirect co-culture, Trans-5 and 10 worms). And, the cells with 1×10^6 cells/dish were cultured within 60φ culture dish for 18 h with 5 ng/ml LPS for CS-TPXs functional study. Each CS-TPX was treated with equally at 100 ng/ml of concentration. The cells and cell culture supernatants were then harvested for further analysis.

3. Flow Cytometry

Harvested cells were washed with PBS containing 0.05% NaN_3 and then stained with FITC-CD40 (BD-553790, BD Biosciences, USA), anti-CD80 (BD-553790), anti-CD86 (BD-553692), anti-TLR2 (sc-52736, Santa Cruz Biotechnology, USA), TLR4 (sc-13591), PE-PD-L1 (12-5982-81, eBioscience, USA) and FITC-PD-L2 (11-9972-81) monoclonal antibodies. Cells were analyzed with a FACSCalibur multicolor flow cytometer (Becton-Dickinson, USA) and electric fluorescence intensity was analyzed using the CellQuest software (Becton-Dickinson) as well as Flowjo7.6.2.

4. Nitric oxide (NO) quantification

A spectrophotometric determination for nitrite (NO_2^-) which called Griess assay was used to assess the NO production levels within the cell culture supernatants (68), I was using modified-Griess regent (Sigma, G4410, USA) that can detect 0.43-65 μM of nitrite. Briefly, equal volumes of Griess reagent and each group's supernatant were mixed and incubated, respectively. After 15 min of incubation at room temperature, absorbances were read at 540 nm. Concentration was determined according to a standard curve of defined concentration of sodium nitrite solution and griess solution mixture.

5. Enzyme-linked immunosorbent assay (ELISA)

Cytokines in culture supernatant such as TNF-α, IL-6, IL-10 and TGF-β were measured by ELISA using commercial kits (e-Bioscience) according to the manufacturer's instructions. 1X culture supernatant was used to detect each amount of cytokines and loaded on capture antibodies coated plate for 2 h. And after 1 h of reaction with detection antibodies, anti-mouse IgG HRP conjugate reaction was done for 30min. Finally, reaction with substrate solution TMB and HRP was carried out for 10min. Each cell culture supernatants was acidified with 1N HCl and then neutralized with 1N NaOH for activation of inactivated TGF-β. And 5 times of washing with PBST were carried out to get rid of non-specific interaction between antibodies and antigens.

6. Identification of *C. sinensis* TPx (CS-TPX)

To clone a TPX gene from *C. sinensis*, gene specific primers (F-TPX: 5'-ATGGCTCTCCTGCCGAAC-3'; R-TPX: 5'-GTTAACGGACGAGAA ATA-3') were designed based on the nucleotides sequence of TPX from

Opisthorchis viverrini (*O. viverrini*, Genbank accession number EU376958). cDNA of *C. sinensis* was synthesized using Reverse Transcription System (Promega, USA). The RNA was loosen at 72℃ for 10 min and then mixed with RTase and Oligo$(dT)_{15}$ primer, this reaction raised at 42℃ for 15 min. The resultant cDNA was amplified by using primers for TPX under following condition: denaturation at 95℃ for 30 sec, annealing at 50℃ for 30 sec and 10 sec elongation at 72℃ for 30 cycles. The PCR products of the expected size were cloned using the pGEM®-T Easy vector (Promega, USA) in *E. coli* DH5α cells (RH618, RBC Bioscience, Taiwan) and analyzed for incomplete *C. sinensis* TPX sequences by gene specific primers and vector-originated sequences (Macrogen Inc., Korea).

7. Full sequence finding of CS-TPX and phylogenetic tree analysis

The partial sequence of the CS-TPX was used to design primer for 5' and 3' rapid amplification of cDNA ends (RACE)-PCR. The RACE-PCR was done with SMART™ RACE cDNA Amplification Kit (634914, Clontech, Japan). Gene specific primer for 3' (5'-ATGGCGATGTGTGCTCA GCGAATTGGAA-3') and Universal Primer Mix A (UPM) were reacted with 3′ RACE-ready cDNA to disclose unknown 3' ends. And gene specific primer for 5' (5'-TCTGTTGGACAGACGAACGTGAAG TCCA-3') and UPM were reacted with 5′RACE-ready cDNA to disclose unknown 5' ends. The PCR reactions were performed according to the manufacturer's protocol with the Advantage® 2 PCR kit (639206, Clontech). The 3' and 5' RACE-PCR products were cloned in the pGEM®-T easy vector in *E. coli* DH5α cells and sequenced. Full sequence of CS-TPX was deposited in Genbank with the accession number HQ216221 (ADN65138.1 for protein ID). The BLAST search program at NCBI and ClustalW program were used to compare

multiple sequence alignments of TPXs from other species.

8. Cloning and expression of CS-TPX open reading frame (ORF)

CS-TPX specific primers were designed which incorporated with *Bam*HI and *Hind*III for the cloning of entire coding regions of TPX cDNA with pQE30 vector. Primer sequences used to cloning for full TPX described in Table 1. The PCR was performed under following condition: denaturation at 95℃ for 30 sec, annealing at 55℃ for 30 sec and 10 sec elongation at 72℃ for 30 cycles. PCR products of the expected size were cloned in the pGEM®-T easy vector in *E. coli* DH5α cells and analyzed the sequence. And the multiplied PCR products were restriction digested with *Bam*HI • *Hind*III and subcloned into pQE-30 vector (Qiagen). The resulting recombinant plasmid was then transformed into *E. coli* M15 cells and CS-TPX inserted colonies were found by gene derived as well as vector derived restriction enzymes.

For protein expression, each CS-TPXs transformed into M15 *E. coli* cells was grown in LB medium containing 100 μg/ml ampicillin and 25 μg/ml kanamycin until the $O.D_{600}$ reached to 0.5 ~ 0.7 at 37℃. Soluble CS-TPX protein was induced with 1mM IPTG under 37℃ for 4 h cultivation. Expression of protein was checked in 12 ~ 15% SDS-PAGE gel running with coomassie blue staining.

9. Protein structure prediction

Three dimensional structures of CS-TPXs were predicted via Protein Homology/analogY Recognition Engine V 2.0 (Phyre2, http://www.sbg.bio.ic.ac.uk/phyre2/html/page.cgi?id=index). The program uses alignment of hidden Markov models via HHsearch to significantly improve accuracy of alignment and detection rate (69). For intensive

prediction for structural difference between CS-TPX T44 and T41, SWISS-MODEL (http://swissmodel.expasy.org/) provided from Swiss Institute of Bioinformatics was utilized (70).

10. Cloning of mutant and deletional CS-TPXs

Active cysteine residue inactivated mutants were generated using the full sequence of the wild type TPX as a template and mutations were introduced via PCR-based site directed mutagenesis. Primers for mutant CS-TPX and deletional CS-TPXs described in Table 2. Hence, non-mutagenic full sequence of TPX external primers was used for mutagenesis of cysteine residue conversion into glycine at 48 and 169 amino acid residues.

C48/G and C169/G mutated template were mutated by external full TPX primers and C48/G as well as C169/G primers, respectively. Each PCR fragments was ligated via recombinant PCR method. And deletional mutant of TPX templates was produced by PCR with Full TPX F and appropriate R primers described in Table 2. Each templates of small CS-TPXs directly cut by *Bam*HI / *Hind*III at 37℃ for overnight and then ligated with pQE30 vector. The pGex-6p-1 vector (GE Healthcare, USA) was used for CS-TPX T38 cloning and expression which is introduced into vector by *Bam*HI / *Eco*RI cutting and ligation. Ligated plasmids were transformed into *E. coli* M15 for pQE30 and BL21 for pGex-6p-1.

11. Purification of recombinant CS-TPX

After induction, bacteria were harvested by centrifugation at 5000 rpm for 20 min and resuspended by imidazole-containing lysis buffer for pQE30 vector inserted M15 cells (10 mM imidazole, 500 mM NaCl, 50 mM NaH_2PO_4, pH 8.0) with 1 mg/ml of lysozyme and kept in ice for 30 min.

Buffer lyzed protein was collected by centrifugation at 13,500 rpm for 30 min and then purified on Ni-NTA Superflow Columns (30622, Qiagen) according to manufacturer's protocol. Bacterial lysis buffer (Pierce) and Tris buffer pH 7.2 were mixed equally for lysis of pGex-6p vector-inserted BL21 cells with 1mg/ml lysozyme. Glutathione agarose beads for binding of GST fusion protein were used for efficient elution of GST-T38 protein. Elution buffer containing imidazole as well as reduced glutathione were dialyzed by PBS using 3 kDa Amicon® ultra-4 centrifugal filter (Millipore, USA). After filtration with a 0.2-μm syringe filter for sterilization, purified protein was quantified by Bradford assay (Bio-Rad, USA) and stored at 4℃ until use.

12. Production of anti-CS-TPx antibody

Polyclonal anti-sera against recombinant CS-TPX was produced in BALB/c mice upon immunization with 20 μg of recombinant CS-TPX protein in each injection at 3-week intervals. Primary immunization was induced with Freund's complete adjuvant (Sigma) and two subsequent immunizations were done with Freund's incomplete adjuvant (Sigma). At 4 weeks after last immunization, anti-CS-TPX poly sera were collected after the heart puncture of mice.

13. Western blotting

The various *C. sinensis* originated antigens (CA, ESP, EA) and recombinant CS-TPX were separated by 12% SDS-PAGE, and transferred to a PVDF membrane (Millipore, USA). Anti-CS-TPX sera were used to detect CS-TPX from the antigens at 1:1,000 dilution with 5% skim milk and 0.05% Tween 20-containing tris-buffered saline pH 7.4 (TBST) under 4℃ for overnight. After washing 3 times for 20 min with TBST, anti-mouse-IgG

conjugated with horseradish peroxidase (HRP) (Dako, Denmark) were used at 1:2,000 dilution for 1 h at room temperature.

For relative immune-blotting analysis of CS-TPXs-treated RAW264.7 cells were lysed by RIPA buffer containing 1 mM PMSF, sodium vanadate for 30 min on ice. Lysates were loaded on 10% SDS-PAGE gel and then transferred on PVDF membrane. Antibodies to phosphorylated and total ERK, JNK, p38, MyD88, IκB-α, p65, p50 and actin (Santa Cruz Biotechnology, USA) were used at 1:1,000 dilution 4℃ for overnight. After washing 3 times for 20 min with TBST, specific secondary IgG conjugated with HRP were used at 1:2,000 dilution for 1 h at room temperature. Each membrane washed again 3 times for 20 min with TBST and then visualized by ECL^{TM} Western blotting detection reagents (GE healthcare). The mean intensity between groups were analyzed by Image J program which is available online (http://imagej.nih.gov/ij/).

14. Animals and *C. sinensis* infection

Five week-old male CBA/N mice were purchased from SLC Inc. (Hamamatsu, Japan) and maintained in ABL-2 (animal bio-safety level 2) conditions in accordance with institutional and national guidelines. For *C. sinensis* infection, mice were infected orally with 30 metacercariae of *C. sinensis* and maintained without any treatment for 4 weeks. The experiments were approved and conducted in accordance with the guidelines established by the Institutional Animal Care and Use Committee (SNU-100117-1) and Institutional Biosafety Committee (SNUIBC-091127-1).

15. Immunolocalization of CS-TPX

C. sinensis adult worms or liver tissue from CBA mice infected with *C.*

sinensis (4 weeks) were fixed in 10% formaldehyde and embedded in paraffin blocks. Sections were made 5 μm thicknesses. The sections were deparaffinized in the xylene and hydrated in a series of ethyl alcohol. And then the sections were treated with 3% H_2O_2-containing methyl alcohol for 10 min. Commercial immune-detection kit (VECTOR) was used according to the manufacturer's instructions. Anti-CS-TPX mouse sera were treated with 1:500 dilution in PBS and normal mouse sera were treated as a isotype control and incubated at 4℃ for overnight. Immunohistochemical staining with polyclonal antibodies to TPX was carried out using the DAB substrate kit for peroxidase (Vector Laboratories, USA) according to the manufacturer's instructions.

16. TLR-GST Pull-down assay

The TLR2-GST, TLR-4-GST fusion protein (ab112361 and ab112362, abcam) was loaded on PBS equilibrated glutathione beads as instructed by the manufacturer, separately. Three hours of post binding between TLRs and GST beads, recombinant wild type CS-TPX and T44 proteins were incubated at 4℃ for overnight. Nonspecific binding was removed by 5 times of washing step with PBS and then beads bound GST complexes were eluted with 50mM reduced glutathione. Eluted proteins were separated by 10% SDS-PAGE and α-6xHis tag as well as α-GST specific proteins detection.

17. Statistical analysis

Statistical analysis was performed by using an independent samples by student T-test. Less than 0.05 of P value was considered as statistically significant. Data were represented by mean + standard error using Prism 5.0 software (GraphPad Software, Inc., USA)

Table 2. Sequence of primers used for site-directed mutagenesis and deletional mutant of CS-TPXs.

Name	Direc-tion	Primer Sequence	Product size (bp)
Full TPX (external)	**F** **R**	AA-GGATCC-ATGGCTCTCCTGCCG CA-AAGCTT-GTTAACGGACGAGAAATA	585
mTPX (C48/G)	**F** **R**	GACTTCACGTTCGTCGGTCCAACAGAGTTGATT AATCAACTCTGTTGGACCGACGAACGTGAAGTC	144 441
mTPX (C169/G)	**F** **R**	CAACATGGCGATGTGGGTCCAGCGAATTGGAAG CTTCCAATTCGCTGGACCCACATCGCCATGTTG	507 78
T55	**R**	CA-AAGCTT-CTA-GAAAGCAATCAACTCTGT	165
T53	**R**	AC-AAGCTTAATCAACTCTGTTGG	159
T50	**R**	AC-AAGCTTTGTTGGACCGACGAA	150
T47	**R**	AC-AAGCTTGACGAACGTGAAGTC	141
T44	**R**	AC-AAGCTTGAAGTCCAGTGGGTA	132
T41	**R**	AC-AAGCTTTGGGTAGAACAGCAA	123
T38	**R**	CT-AAGCTTCTACAGCAAAATGACGTATTT	114
PGex T38	**F**	AA-GGATCC-ATGGCTCTCCTGCCG	114
PGex T38	**R**	CA-GAATTC-CTA-GAAAGCAATCAACTCTGT	114

RESULTS

1. *C. sinensis* adult worms induced the morphologic change of RAW 264.7 cells into spindle-like shape.

To observe the effect of *C. sinensis* ESP on the morphology of RAW264.7 cells, cells were co-cultured with worms with or without LPS. The morphology of RAW264.7 cells were transformed as spindle-like cells when 10 worms were co-cultured directly with cells (10 worms, Fig. 1B) or cultured in a transwell (Trans-10 worms, Fig. 1C). There were few eggs in 10 worms group but not in Trans-10 worms group since a size of egg is bigger (30 um) than a pore of transwell membrane (8 um).

Treatment of 10 ng/ml LPS brought about major morphologic transformation of RAW264.7 cells. Sizes of nuclei as well as cytoplasm were bigger than those of control groups and cytoplasm spread the field widely like chicken eggs (Fig. 1D). In order to examine how *C. sinensis* worms survive in harmful environment induced by inflammatory stimuli, LPS was added to 10 worms (LPS/10 worms) and Trans-10 worms (LPS/Trans-10 worms) groups. Interestingly, lots of eggs were laid in LPS/10 worms group, which was not seen in 10 worms group. And morphologies of cells were differed from LPS group, and more spindle-like and less spread cells were observed in LPS/10 worms group (Fig. 1E). The cells in LPS/Trans-10 worms group showed most distinguished morphology change than those in LPS group. Spindle-like morphology was observed in this group and the chicken egg morphology were not seen by 10 worms co-culture within transwell (Fig. 1F). Therefore, whether LPS stimuli presented or not, *C. sinensis* ESP induces morphologic transformation of RAW264.7 cells into spindle-like shapes and these changes represented not only direct but also indirect co-cultured groups.

2. Up-regulation of surface expression of CD86 and TLR-4 in RAW264.7 cells by *C. sinensis* co-culture

To demonstrate the signal from *C. sinensis* ESP to RAW264.7 macrophage cell line, the expression of cell surface markers were observed by flow-cytometric analysis. As shown in Figure 2A and B, cells of Trans-5 and 10 worms groups showed up-regulated CD86 level while CD80 level was not affected significantly. Moreover, antigens from *C. sinensis* were detected by TLR4 rather TLR2 and the expression was increased as the number of worms increased (Fig. 2A and 2B).

However, ESP antigen of *C. sinensis* did not affect the expression of surface markers of LPS-treated cells. Changes of expression levels by these treatments were unstable but fluctuated. Figure 2C showed that the expression level of TLR2 was down-regulated by LPS/5 and 10 worms and LPS/Trans-10 worm groups but it was not statistically significant.

3. Down-regulation of LPS-induced NO and IL-6 production by *C. sinensis* worm co-culture

LPS-induced NO production was down-regulated by all of the worm co-culture groups (Fig. 3A) and NO was not detected when worms were co-cultured without LPS (data not shown). Likewise, IL-6 level by LPS was down-regulated by all worm co-culture groups (Fig. 3B).

4. Up-regulation of anti-inflammatory cytokines, IL-10 and TGF-β, by *C. sinensis* worm co-culture

The production of anti-inflammatory cytokines IL-10 and TGF-β was analyzed by ELISA. Unlike with pro-inflammatory cytokines, IL-10 and TGF-β were upsurged by worm co-culture but the amounts of produced

cytokines were not different irrespective of LPS treatment (Fig. 4A and 4B). Produced amount of IL-10 was more synergically increased by LPS treatment in LPS/Trans-10 worms group than other groups (Fig. 4A). Tendency between the number of worm and amount of TGF-β increased more in LPS/Trans-10 group than other groups but had not significant (Fig. 4B).

5. Expression and purification of recombinant CS-TPX

585bp of whole coding region of *C. sinensis* TPX was polymerized by PCR as shown in Figure 5A. M15 cells transformed with pQE-30-TPX plasmid were induced to produce native recombinant TPX protein under 1mM IPTG 37℃ for 4h of cultivation. As shown in Figure 5A, the emphasized protein band with the expected size (24kDa) was detected on the 12% SDS-PAGE gel (Fig. 5B, lane 2) compared to non-induced *E. coli* pellets (Fig. 5B, lane 1). After the confirmation of 6xHis-tagged TPX protein expression by western blotting with α-6xHis-tag antibody (Fig. 5C), induced TPX was purified using the Ni-NTA columns (Fig. 5B, lane 3).

6. Sequence analysis of CS-TPX and phylogenetic tree

The 728bp of CS-TPX cDNA was disclosed by RACE-PCR. Whole cDNA nucleotides contained an open reading frame of 195 amino acids and molecular mass is 21.9kDa, hypothetically. There were two conserved VCP motifs at 47 (FYPLDFTFVCPTELIA) and 168 (VCPA) amino acid positions which indicated that typical 2-Cys peroxiredoxin active sites (Fig. 6, red box). The CS-TPX encoded had higher identity to TPX from trematode parasites such as *S. mansoni* (XP_002577886.1) 73% and *F. hepatica* (CAA06158.1) 72% than those from *Caenorhabditis elegans* (NP_001122604.1) 59%, *Taenia solium* (ACM89281.1) 55%, *Leishmania major* (AAC79432.1) 60% and

Homo sapiens (NP_002565.1) 57% (Fig. 6). It showed 97% amino acids identity to *O. viverrini* TPX (EU376958) (data not shown). Overall, the high matching score between different organisms indicated that *C. sinensis* TPX is conserved among the parasites. Phylogenetic analysis of CS-TPX was most similar to TPXs of *O. viverrini* and schistosomes (Fig. 7) and CS-TPX was in different clade with TPXs from mouse, rat and human (Fig. 7)

7. Localization of the CS-TPX

In order to identify existence of TPX in antigens of *C. sinensis*, proteins interacting with anti-TPX poly sera were visualized from the *C. sinensis* antigens via western blotting. Immuno-blotting result revealed that CA, ESP and egg antigen of *C. sinensis* contained TPX at expected size of 24 kDa (Fig. 5D).

Furthermore, to localize CS-TPX at worm itself, immuno-histochemistry was done with *C. sinensis* infected liver tissue of CBA mouse. Isotype control anti-mouse poly sera did not bind to any mouse liver tissue as well as worm body (Fig. 8A). However, CS-TPX exhibited wide expression pattern throughout the body of worm, especially in the tegument, ventral sucker, eggs as well as excretory products of the worm (Fig. 8B-D). Moreover, the CS-TPX was also detected in the bile duct epithelial cells in close proximity to the worms.

8. CS-TPX inhibited LPS-induced TLR4 expression and production of inflammatory cytokines in RAW264.7 cells

To confirm whether CS-TPX is an effective anti-inflammatory protein or not, LPS-induced TLR4, CD40, CD80, CD86, PD-L1 and PD-L2 expression levels were detected by flow-cytometry (Fig. 9). Interestingly, wild type of

CS-TPX partially down-regulated expression of LPS-induced TLR4 (Fig. 9A-C). However, expression levels of co-stimulatory molecules such as CD40, CD80, CD86, PD-L1 and PD-L2 were not affected (Fig. 9A).

In order to determine direct interaction between TLR and TPX, GST pull-down assay was carried out with TLR2 and TLR4-GST fusion protein. Interestingly, TPX bound to both TLR2 and TLR4 (Fig. 9D).

Down-regulatory effects of CS-TPX in LPS-induced inflammatory mediators were investigated as in CS-ESP experiment. As shown in Figure 10A-C, production of NO, TNF-α, IL-6 were partially decreased by LPS and CS-TPX co-treatment in RAW264.7 cells. Anti-inflammatory cytokine, IL-10 levels were increased (Fig. 10D) but TGF-β was not detected in LPS and CS-TPX co-treated cells (data not shown). Thus, LPS-induced activation of RAW264.7 cells were alleviated by CS-TPX treatment and it could be mediated by TLR4-CS-TPX direct interaction.

9. The ability of CS-TPX to reduce LPS-induced activation was independent of its antioxidant activity

In order to check whether the antioxidant activity of CS-TPX was related with the macrophage regulatory effect, mutant forms of CS-TPX was produced. Redox-active C48 and C168 residues to detoxify H_2O_2 of CS-TPX were replaced with glycine each by site-direct mutagenesis and named CS-mTPX (Fig. 11A, B). As a result of these replacements, CS-mTPX was deprived of reactive center. The size of expressed CS-mTPX by *E. coli* system was not changed by mutation and efficiently purified under native condition (Fig. 11C).

Protein 3D structure predictions results of CS-mTPX revealed loosen 3' terminal than wild type CS-TPX but maintained tighten up 5' end (Fig. 12A,

B).

To confirm whether CS-mTPX has effective anti-inflammatory protein or not even without enzymatic activity, LPS-induced TLR4, CD40, CD80, CD86, PD-L1 and PD-L2 expression levels were detected (Fig. 13). Same as above, cysteine residue inactivated CS-mTPX down-regulated expression of LPS-induced TLR4 (Fig. 13A, B, C). However, co-stimulatory molecules such as CD40, CD80, CD86, PD-L1 and PD-L2 expression levels were not affected (Fig. 13A).

LPS-induced productions of NO, TNF-α, IL-6 were decreased by CS-mTPX with same magnitude as CS-TPX does (Fig. 14A-C). Moreover, IL-10 levels were increased (Fig. 14D) but TGF-β was not detected in LPS and CS-mTPX co-treated cells (data not shown). Hence, these results ensured that the CS-TPX mediated suppression of macrophages is independent of its peroxidase activity.

10. T44 is the smallest CS-TPX which exert macrophage regulatory function through their structure of sequence basis

Since CS-mTPX has the regulatory function on LPS-induced RAW264.7 cell activation, it is assumed that the immune regulation effects of CS-TPX is on structural or sequence basis mechanisms. Therefore, cloning for deletional mutant was performed to make the smallest CS-TPX recombinant protein which has intact immune-regulatory function. CS-TPX T55 having full inactivated cysteine residue (FYPLDFTF VGPTELIAF) was set as the start point for sequential production of CS-TPX deletional mutant because T167, T127 CS-TPX has intact immune-regulatory properties as CS-mTPX does in preliminary data (data not shown). Each amino acid sequences of CS-TPXs and vector composition are described (Fig. 15A-C).

Protein 3D structure prediction revealed relatively more stable structure in T55, T53 and T50 CS-TPX which had alpha helices at C terminal (red) than in T47, T44, T41 and T38 (Fig. 16A-G).

Successful expression of T55, T53, T50, T47, T44 and T41 CS-TPXs are shown in 15% of SDS-PAGE and each CS-TPXs are soluble in native condition (Fig. 17A). Because T38 CS-TPX was not expressed at all in pQE30 system, glutathione s-transferase (GST) encoding pGex-6p vector was used to achieve expression of the smallest CS-TPX. 26 kDa GST protein was expressed in supercoiled pGex-6p vector only and T38 CS-TPX inserted vector produced T38-GST protein which has approximately 30 kDa of size (Fig. 17B).

To verify which CS-TPX mutants contained an immune-regulatory region, RAW264.7 cells were treated with LPS and each CS-TPX mutants. Interestingly, LPS-induced expression of TLR4 was down-regulated only by exogenous treatment with T55, T53, T50, T47, T44 CS-TPX but not regulated by T41 and T38 treatment (Fig. 18A-C).

Striking feature of CS-TPXs in LPS-induced productions of NO, TNF-α, IL-6 levels were decreased by T55, T53, T50, T47 and T44 CS-TPX treatment with same magnitude as CS-mTPX did (Fig. 19A-C). Moreover, IL-10 levels were increased (Fig. 19D) but TGF-β was not detected in LPS and small CS-TPXs co-treated cells (data not shown).

Intensive modeling of protein structure via web-based SWISS-MODEL program demonstrated that the T44 CS-TPX had short alpha-helices on 28KDY residue (Fig. 20A) but not in T41 CS-TPX (Fig. 20B). And this 28KDY short alpha-helices was observed in T47, T50, T55 CS-TPX, too (data not shown).

Thus, the smallest CS-TPX having inhibitory activities for macrophage

activation was sequenced and structure-dependent mechanism is possibly dependent on 28KDY which resided in T44 as well as bigger CS-TPX mutants.

11. LPS-negative regulatory effect of CS-TPX was independent on NF-κB

Immunoblotting showed that the expression of main adaptor proteins such as TLR4 and MyD88 were slightly reduced in CS-TPX and T44 groups at 15, 30, 60 min than in LPS treatment group (Fig. 21, 22A). However, expression of IkB-α and NF-κB subunit p65, p50 dimer were not affected by CS-TPX and T44 treatment (Fig. 21, 22B-D). And amount of phosphorylated form of MAPKinase ERK and JNK were not affected, too (Fig. 21, 22EF). Phosphorylated p38 was not detected. Therefore, suppressive property of CS-TPX on LPS-induced activation of RAW264.7 cells was not involved with NF-κB and MAPK signaling in this system.

12. CS-TPX down-regulated LPS-induced TNF-α production from human macrophage-like cell line, THP-1.

Human macrophage-like cell line, THP-1 cells were cultured with CS-TPX and LPS to confirm inhibitory effect of macrophage activation by CS-TPX in human. There was no significant surface expression of TLR-4 by LPS stimulation so that down-regulation of TLR-4 by CS-TPX was not observed (data not shown). However, LPS-induced TNF-α production was decreased by CS-TPX treatment, significantly (Fig. 23).

Blood $CD14^+$ monocytes obtained from a healthy human were sorted and differentiated to macrophages by human M-CSF treatment. However, 100 ng/ml of LPS treatment was inefficient to get fully activated macrophages. And there was no CS-TPX-induced reduction of TLR-4 expression (data not shown). Thus, optimal human *in vitro* experimental condition is necessary to study macrophage inhibitory effect of CS-TPX.

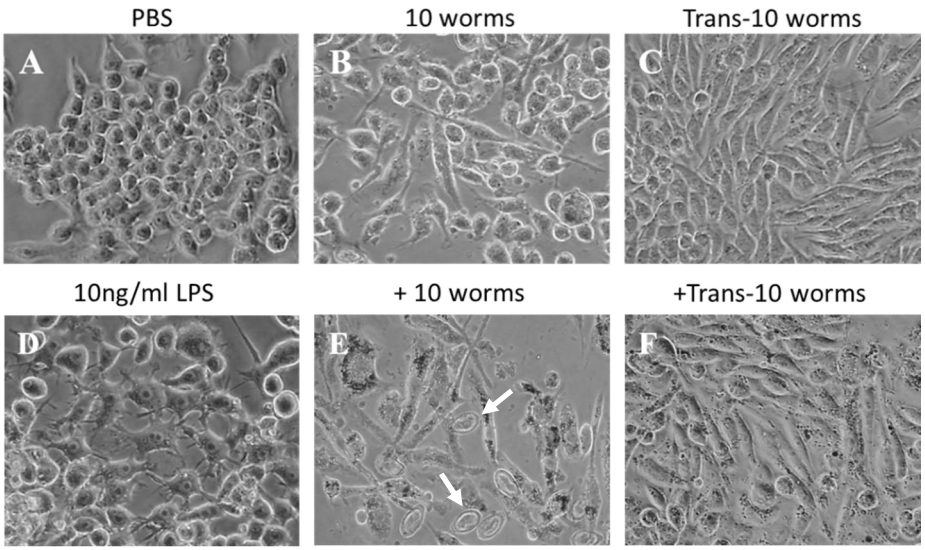

Figure 1. *C. sinensis* ESP changed the morphology of RAW264.7 cells into spindle-like structure. RAW264.7 cells were cultured in 24 well plates (8×10^4 cells/well) with/or without *C. sinensis* adult worms and LPS. Cells were observed under a phase contrast microscope after 72 h of cultivation and images were taken with a digital camera. PBS treated control (A), co-cultured cells with 10 worms (B), co-cultured cells with 10 worms through trans-well (C), 10 ng/ml LPS treated cells (D), LPS and 10 worms co-cultured cells (E), LPS as well as 10 worms co-cultured cells through trans-well (F). Arrows indicate produced eggs. Data represent three independent experiments.

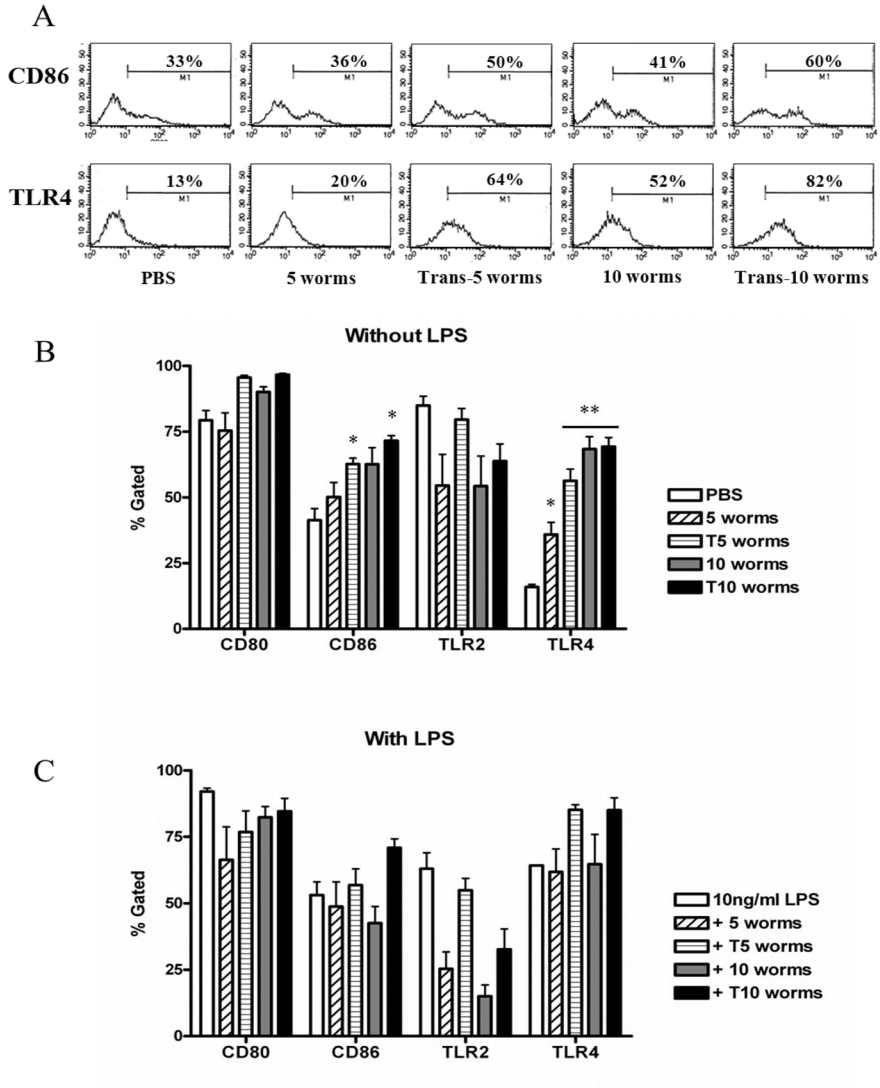

Figure 2. Phenotypic changes of RAW264.7 cells in response to *C. sinensis* ESP. Cells were harvested after 72 h of cultivation and labelled with FITC- or PE-conjugated anti-CD80, CD86, CD40, TLR-4 monoclonal antibodies. CD86 and TLR-4 expression patterns were demonstrated as statistically significant representative data (A). The levels of % gated expression levels were summarized when cells were co-cultured with worms but without LPS (B) or with LPS (C). Data represent the means ± SE of three independent experiments (B). *$P< 0.05$, **$P< 0.01$ (t-test), significantly different from the value obtained in cell supernatants.

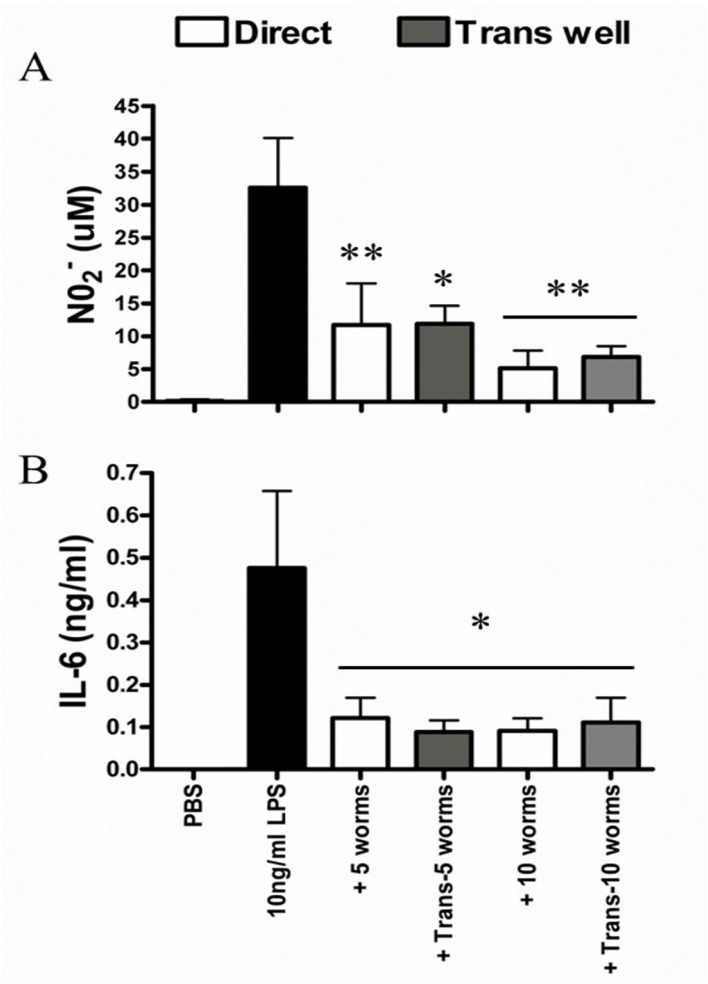

Figure 3. *C. sinensis* ESP regulate LPS-induced nitrite (NO_2^-) and IL-6 cytokine production from RAW264.7 cells. After 72 h cultivation, cell supernatants were collected and nitrite production level was analyzed with modified Griess reagent (A). ELISA was performed to determine produced level of IL-6 (B). Data represent the means ± SE of more than three independent experiments. *$P< 0.05$, **$P< 0.01$ (t-test), significantly different from the value obtained in cell supernatants.

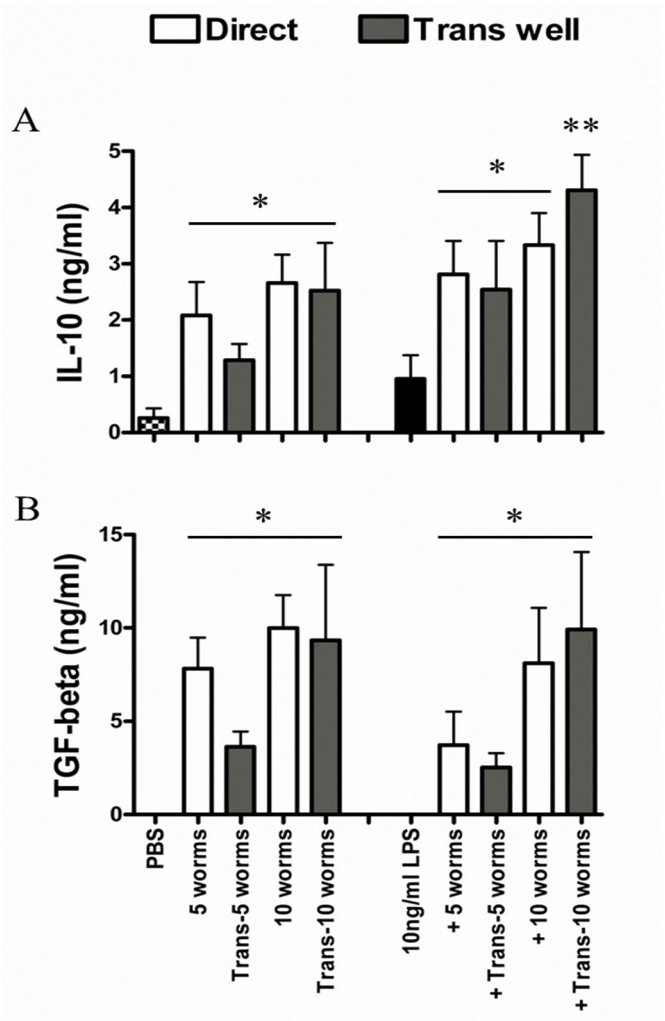

Figure 4. Production of anti-inflammatory cytokines IL-10 and TGF-β from RAW264.7 cells by *C. sinensis* co-culture. After 72 h cultivation, cell supernatants were collected and the levels of IL-10 (A) and TGF-β (B) was analyzed by ELISA. Data represent the means ± SE of more than three independent experiments. *$P< 0.05$, **$P< 0.01$ (t-test), significantly different from the value obtained in cell supernatants.

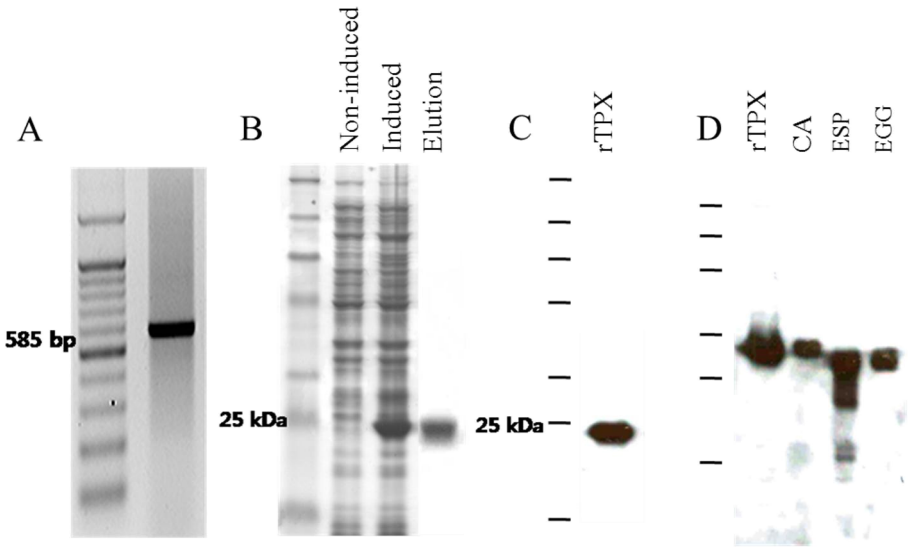

Figure 5. Expression of CS-TPX in *E. coli* system and confirm of anti-TPX poly sera from antigen of *C. sinensis* origin. Proteins were separated on 12% SDS-PAGE gels. (A) Coomasie blue staining results of E. coli lysates. Lane 1 - non-induced control; Lane 2 - induced TPX by 0.1 mM IPTG; Lane - 3, purified TPX by NiNTA column; (B) Western blotting results of recombinant TPX and anti-6x-His tag antibody (1:2000 dilution) ; (C) anti-TPX poly sera epitope confirmation with indicated antigens from *C. sinensis.*

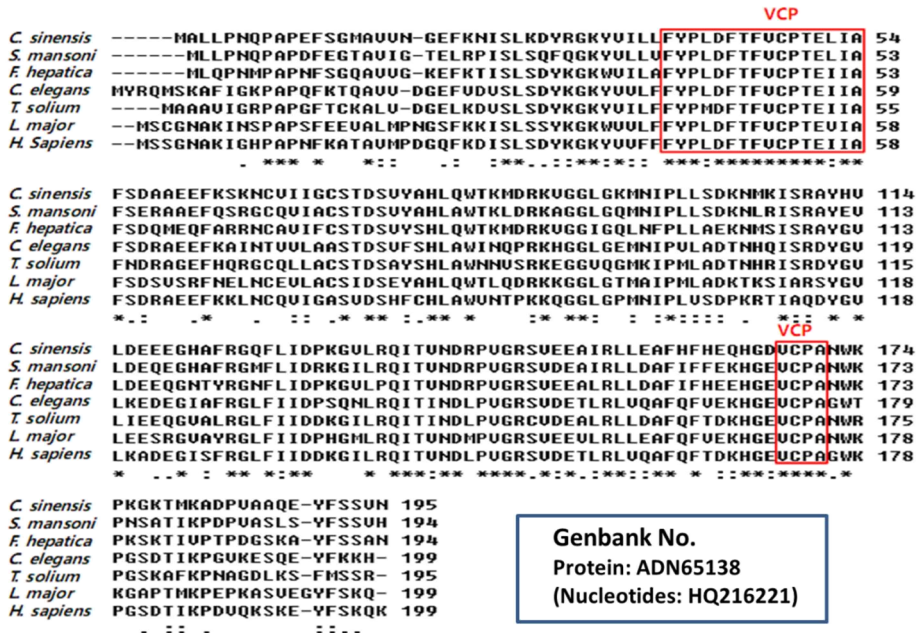

Figure 6. Multiple alignments of the CS-TPX sequences with TPX from other species. *S. mansoni* (XP_002577886.1), *F. hepatica* (CAA06158.1), *C. elegans* (NP_001122604.1), *T. solium* (ACM89281.1), *L. major* (AAC79432.1) and *H. sapiens* (NP_002565.1). Highly conserved regions with cysteine residues are boxed and marked by VCP. Symbols below the sequence indicate identical residues (*), highly conserved residues (:) and moderately conserved residues (.).

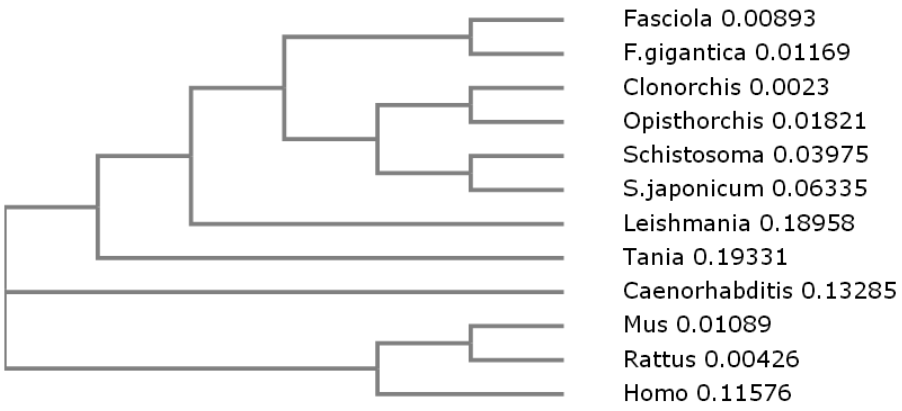

Figure 7. Phylogenetic tree of CS-TPX and other species.

(ClustalW2 : http://www.ebi.ac.uk/Tools/phylogeny/clustalw2_phylogeny/)

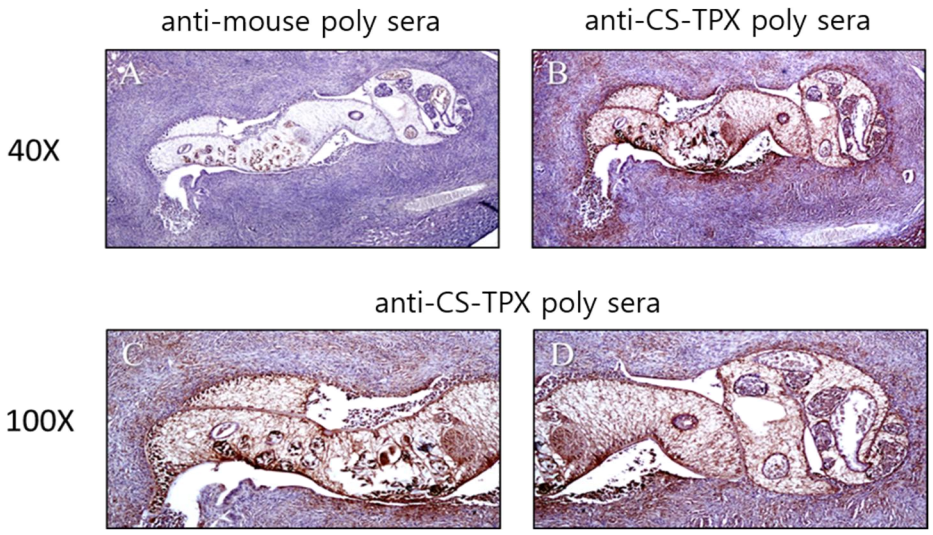

Figure 8. Immunolocalization of CS-TPX at *C. sinensis* adult worm. Immunohistochemistry was done with adult *C. sinensis* in the bile ducts of experimentally infected CBA mice. (A) anti-mouse poly sera (1:200 dilution) was proved as an isotype control, 40X magnification; (B) anti-TPX poly sera (1:200 dilution) was proved, 40X magnification; (C, D) anti-TPX poly sera, 100X magnification.

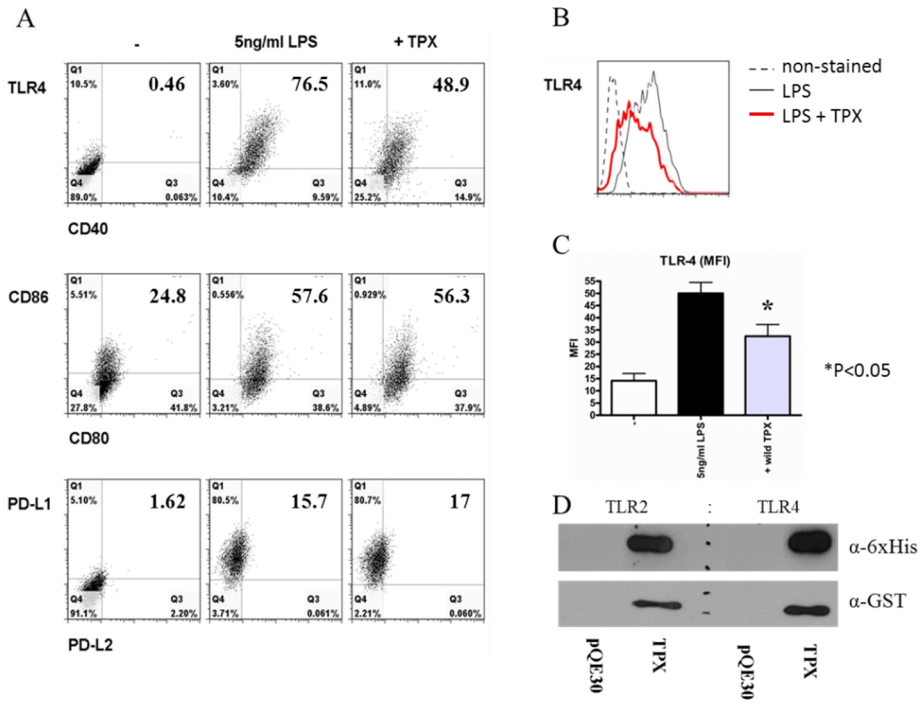

Figure 9. CS-TPX decreases LPS-induced expression of TLR4 and directly binds with TLR2 as well as TLR4. Cells were harvested after 18 h of cultivation and labelled with FITC- or PE-conjugated anti-TLR4, CD40, CD80, CD86, PD-L1 and PD-L2 monoclonal antibodies. The expression patterns of surface markers were demonstrated as two dimensional dot plot (A). The representative results for TLR4 expression by CS-TPX treatment (red-bold line) was shown in histogram (B). Average score for calculated MFI summarized (C). Immunoblotting results for pull-down assay between TPX and GST fusion TLR2/TLR4 protein (D). Data represent the means ± SE of three independent experiments *$P< 0.05$ (t-test), significantly different from the value obtained in cell supernatants.

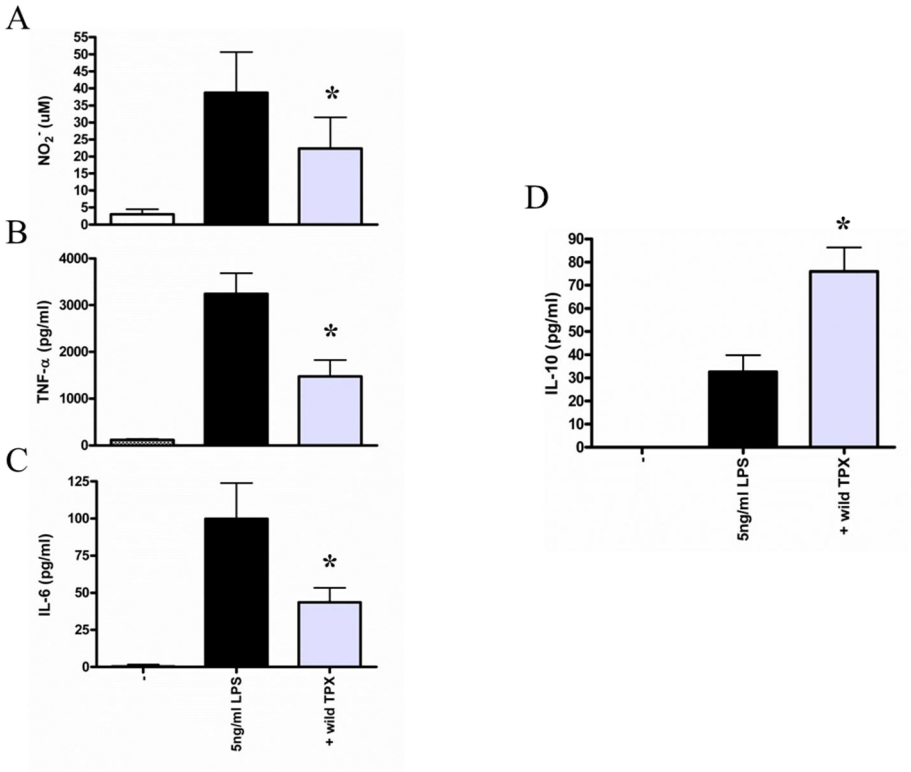

Figure 10. CS-TPX reduces LPS-induced production of NO, IL-6, and TNF-α and increases IL-10 production from RAW264.7 cells. Cell supernatants were collected after 18 h of cultivation and nitrite production level was analyzed with modified Griess reagent (A). ELISA was performed to determine the level of TNF-α (B), IL-6 (C) and IL-10 (D). Data represent the means ± SE of three independent experiments. *$P< 0.05$ (t-test), significantly different from the value obtained in cell supernatants.

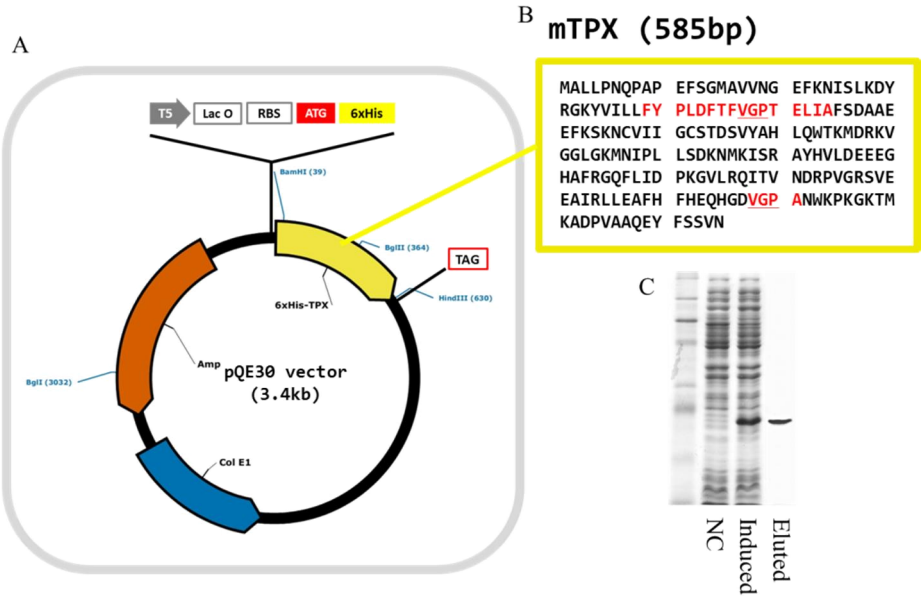

Figure 11. Cloning and purification of mTPX. Diagram for pQE30 vector composition is described (A). TPX sequence both C48G and C169G mutated mTPX is shown (B). M15 cell expressed (C, lane 2) and purified CS-mTPX represented in 12% SDS-PAGE (C, lane 3).

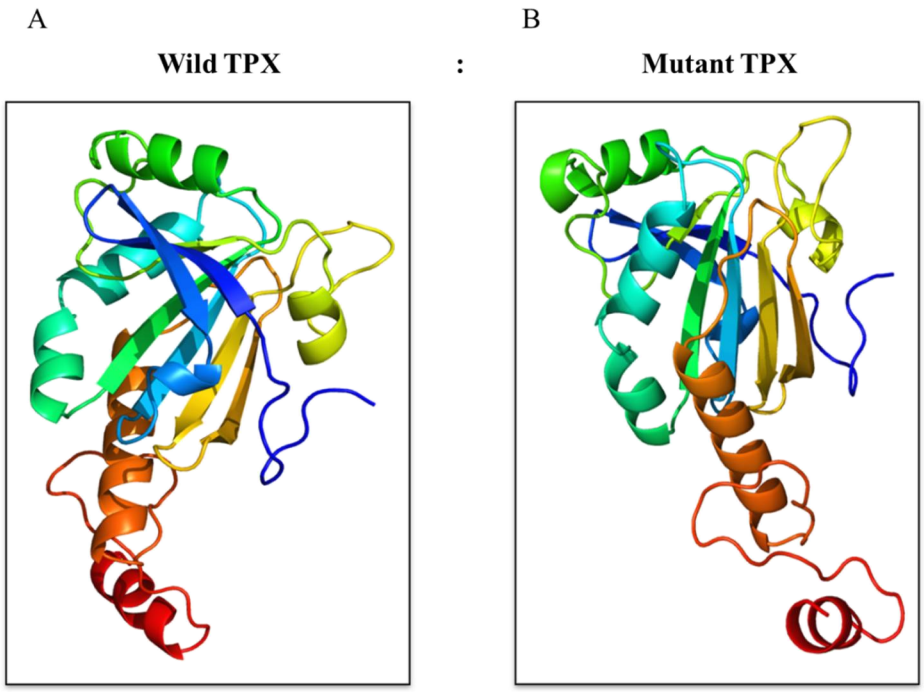

Figure 12. Web-based prediction of CS-TPX and CS-mTPX structures. Three dimensional protein structures were reconstructed by Phyre2.0 (http://www.sbg.bio.ic.ac.uk /phyre2/html/page.cgi?id=index). N-terminal is represented in red color and C-terminal is shown in blue color for CS-TPX (A), and CS-mTPX (B).

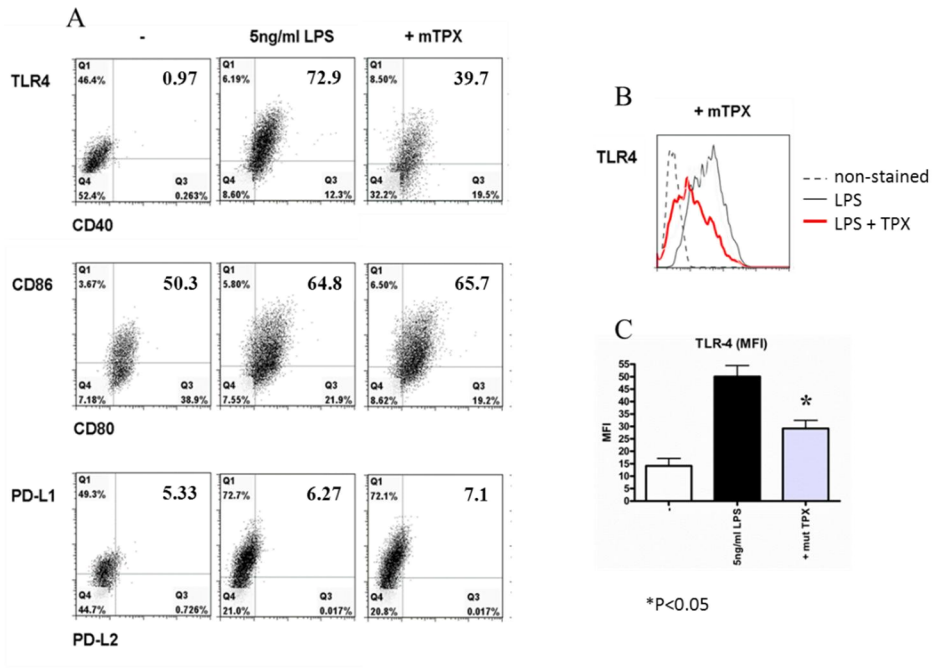

Figure 13. CS-mTPX decreases LPS-induced expression of TLR4 independently with antioxidant activity. Cells were harvested after 18 h of cultivation and labelled with FITC- or PE-conjugated anti-TLR4, CD40, CD80, CD86, PD-L1 and PD-L2 monoclonal antibodies. The expression patterns of surface markers were demonstrated as two dimensional dot plot (A). The representative results for TLR4 expression by CS-mTPX treatment (red-bold line) was shown in histogram (B). Average score for calculated MFI summarized (C). Data represent the means ± SE of three independent experiments *$P< 0.05$ (t-test), significantly different from the value obtained in cell supernatants.

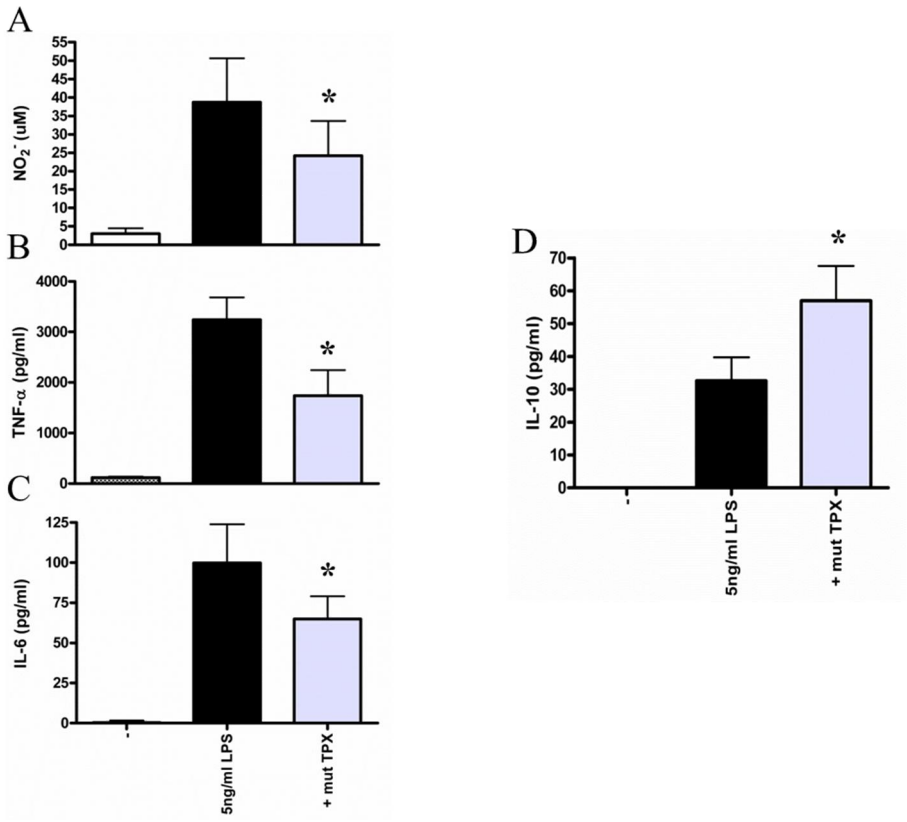

Figure 14. CS-mTPX reduces LPS-induced production of NO, IL-6, and TNF-α levels and increases IL-10 production from RAW264.7 cells independently with antioxidant activity. Cell supernatants were collected after 18 h of cultivation and nitrite production level was analyzed with modified Griess reagent (A). ELISA was performed to determine the level of TNF-α (B), IL-6 (C) and IL-10 (D). Data represent the means ± SE of three independent experiments. *$P< 0.05$ (t-test), significantly different from the value obtained in cell supernatants.

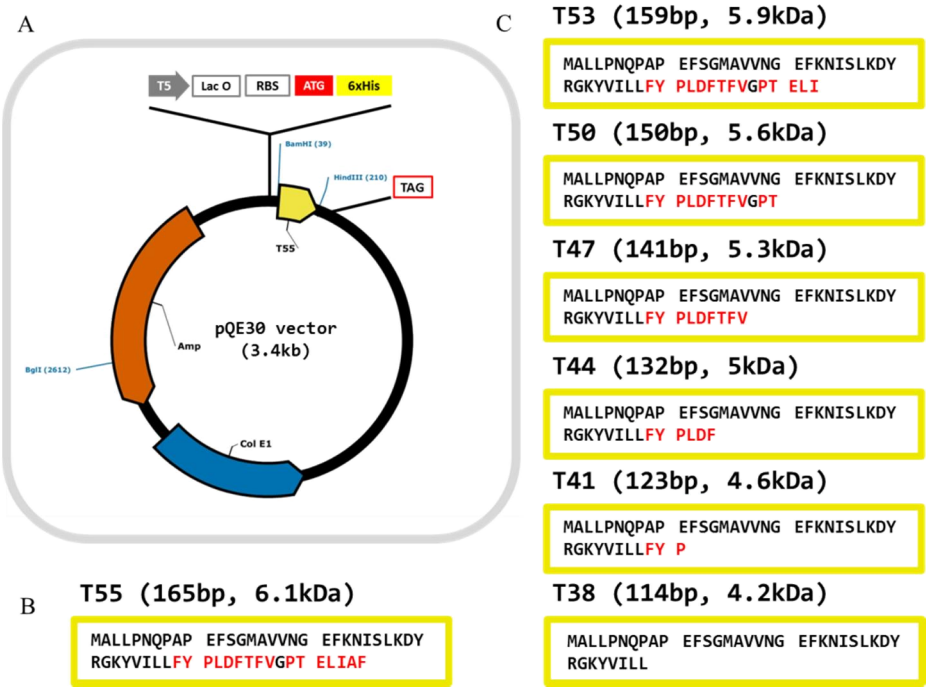

Figure 15. Cloning strategies of deletional mutants. Diagram for pQE30 vector composition is described (A). Sequences of small CS-TPX mutants based on CS-mTPX are shown (B, C).

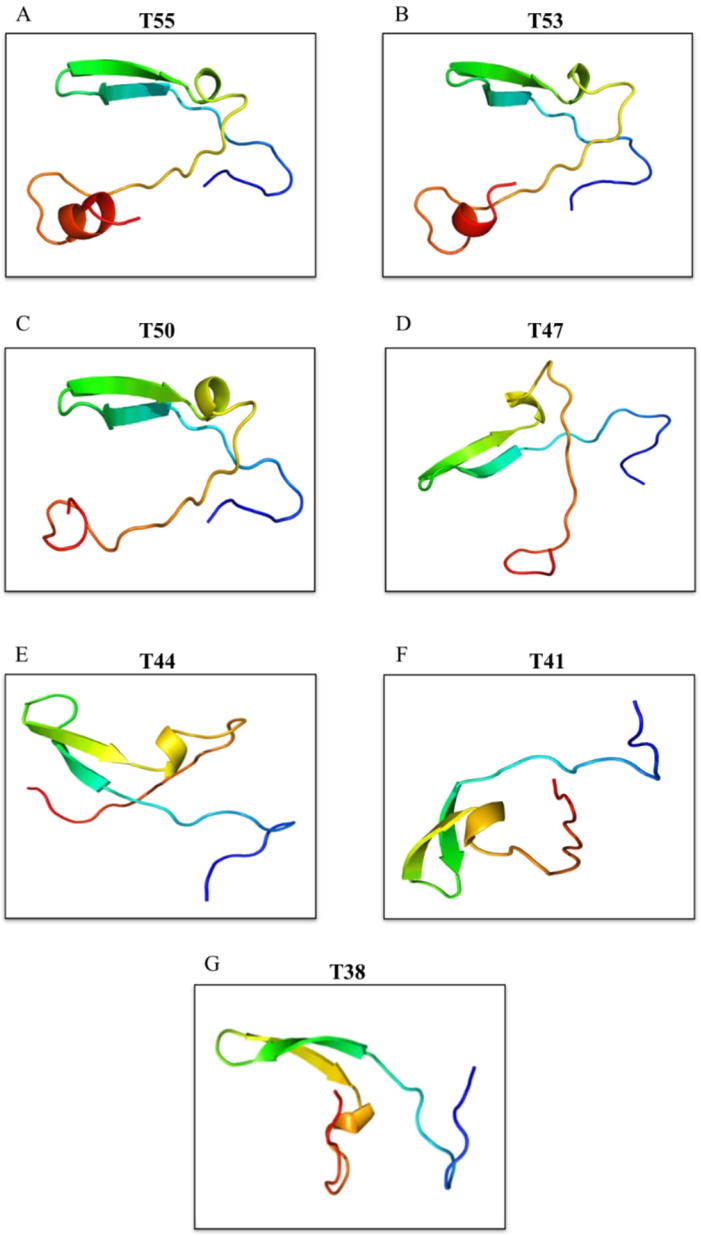

Figure 16. Web-based prediction of smallest CS-TPX structures. Three dimensional protein structures were reconstructed by Phyre2.0 (http://www.sbg.bio.ic.ac.uk /phyre2/html/page.cgi?id=index). N-terminal is represented in red color and C-terminal is shown in blue color for T55 (A), T53 (B), T50 (C), T47 (D), T44 (E), T41 (F), and T38 (G).

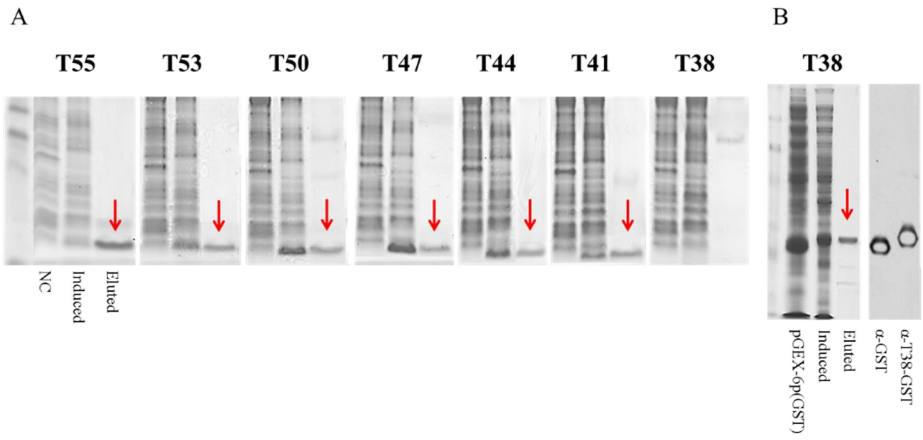

Figure 17. Expression and purification of CS-TPX deletional mutants. M15-inducing deletional CS-TPXs-inserted pQE30 fusion protein were purified and demonstrated in 15% SDS-PAGE gels (A). BL21 inducing T38-inserted pGex-6p fusion protein was purified and confirmed in 12% SDS-PAGE gels. Positive band for a-GST antibody was detected by western blotting (B).

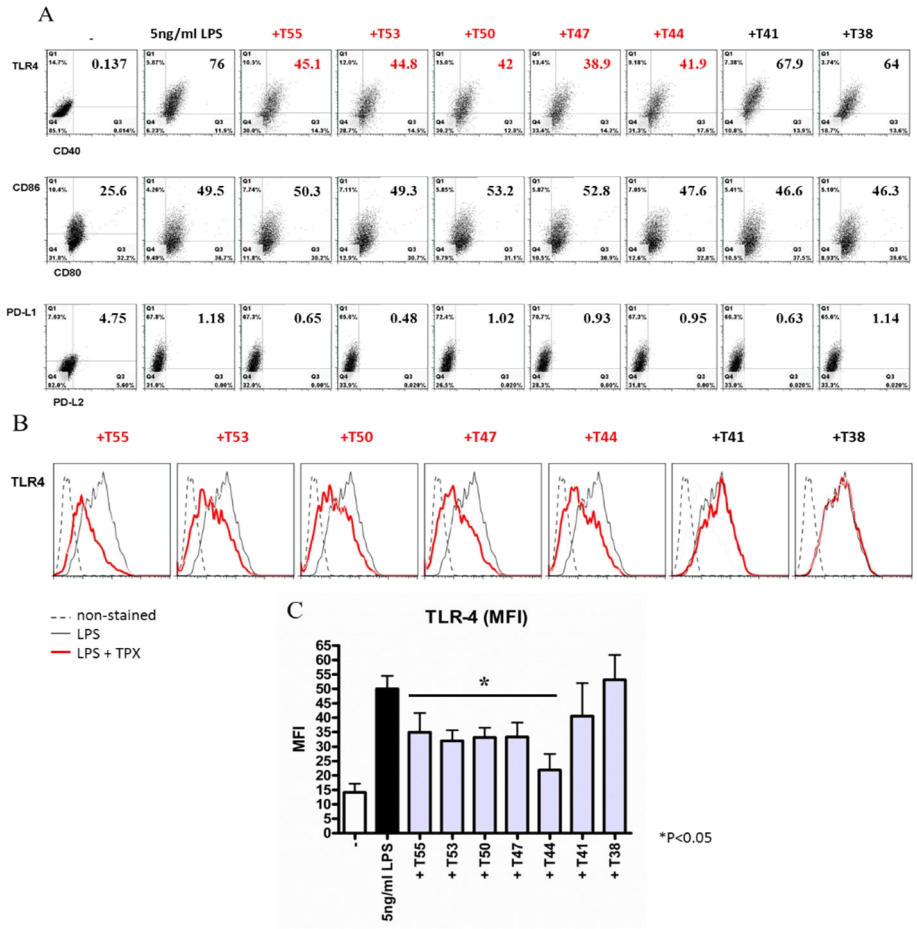

Figure 18. T44 is the smallest CS-TPX that decreases LPS-induced expression of TLR4. Cells were harvested after 18 h of cultivation and labelled with FITC- or PE-conjugated anti-TLR4, CD40, CD80, CD86, PD-L1 and PD-L2 monoclonal antibodies. The expression patterns of surface markers were demonstrated as two dimensional dot plot (A). The representative results for TLR4 expression by small CS-TPX treatment (red-bold line) is shown in histogram (B). Average score for calculated MFI summarized (C). Data represent the means ± SE of three independent experiments *$P< 0.05$ (t-test), significantly different from the value obtained in cell supernatants.

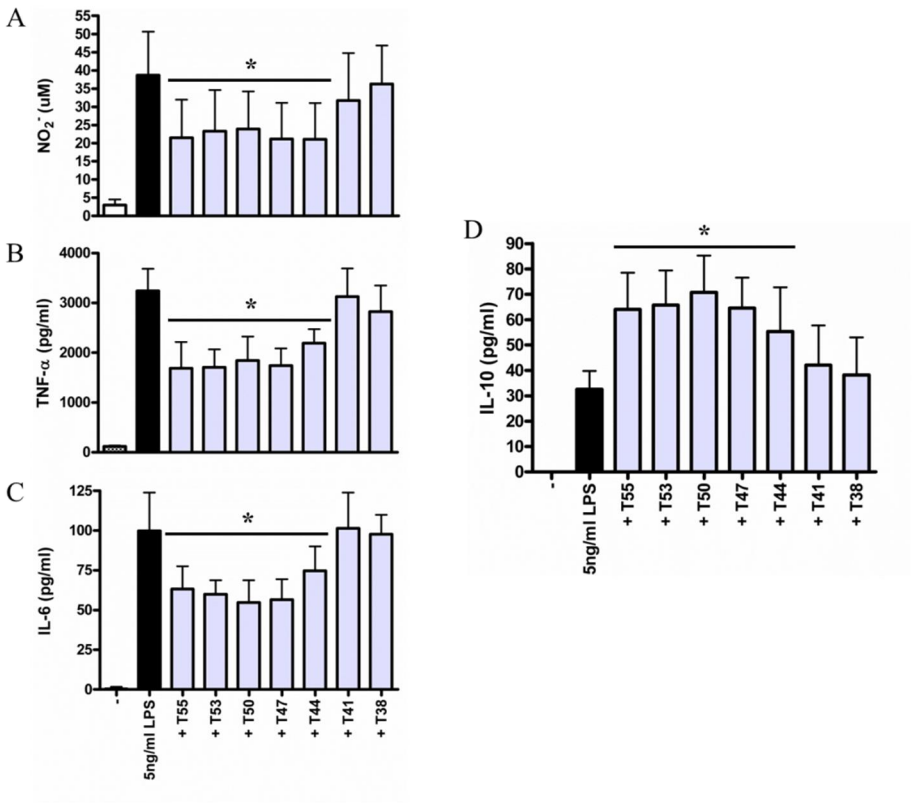

Figure 19. T44 is the smallest CS-TPX that reduces LPS-induced production of NO, IL-6, and TNF-α and increases IL-10 production from RAW264.7 cells. Cell supernatants were collected after 18 h of cultivation and nitrite production level was analyzed with modified Griess reagent (A). ELISA was performed to determine the level of TNF- α (B), IL-6 (C) and IL-10 (D). Data represent the means ± SE of three independent experiments. *$P< 0.05$ (t-test), significantly different from the value obtained in cell supernatants.

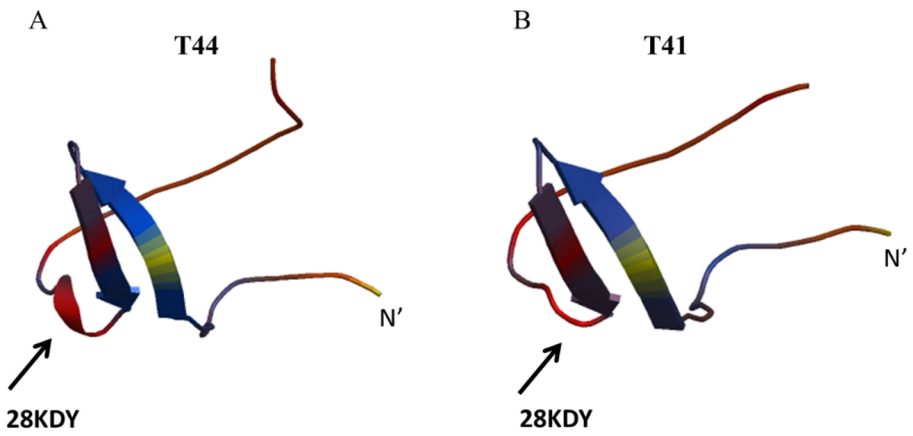

Figure 20. SWISS-MODEL predicted smallest CS-TPX structure is differed between T44 and T41. Three dimensional protein structures were reconstructed by SWISS-MODEL (http://swissmodel.expasy.org/). T44 (A), T41 (B).

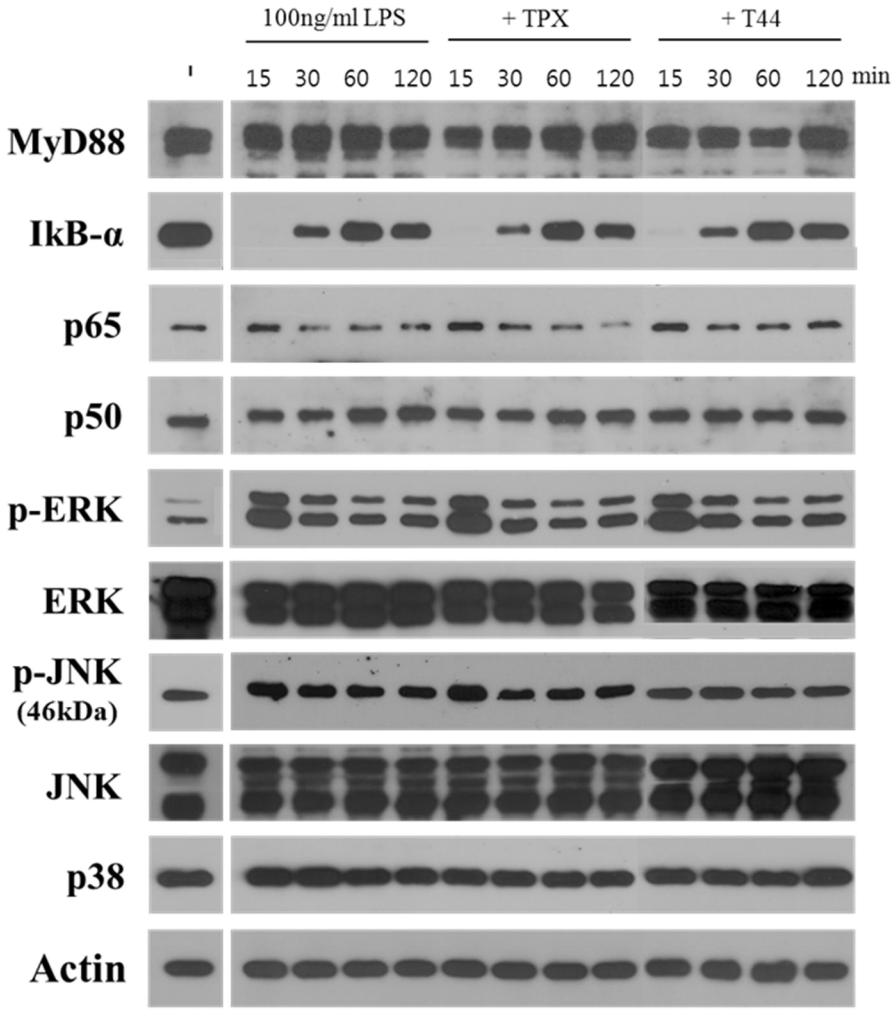

Figure 21. Immunoblotting results of CS-TPXs treated RAW264.7 cells with LPS. The lysates of 1 X 10^6 cell equivalents from each group were immunoblotted with the indicated antibodies. PVDF membranes were stripped and then reproved with different antibodies up to 3 times.

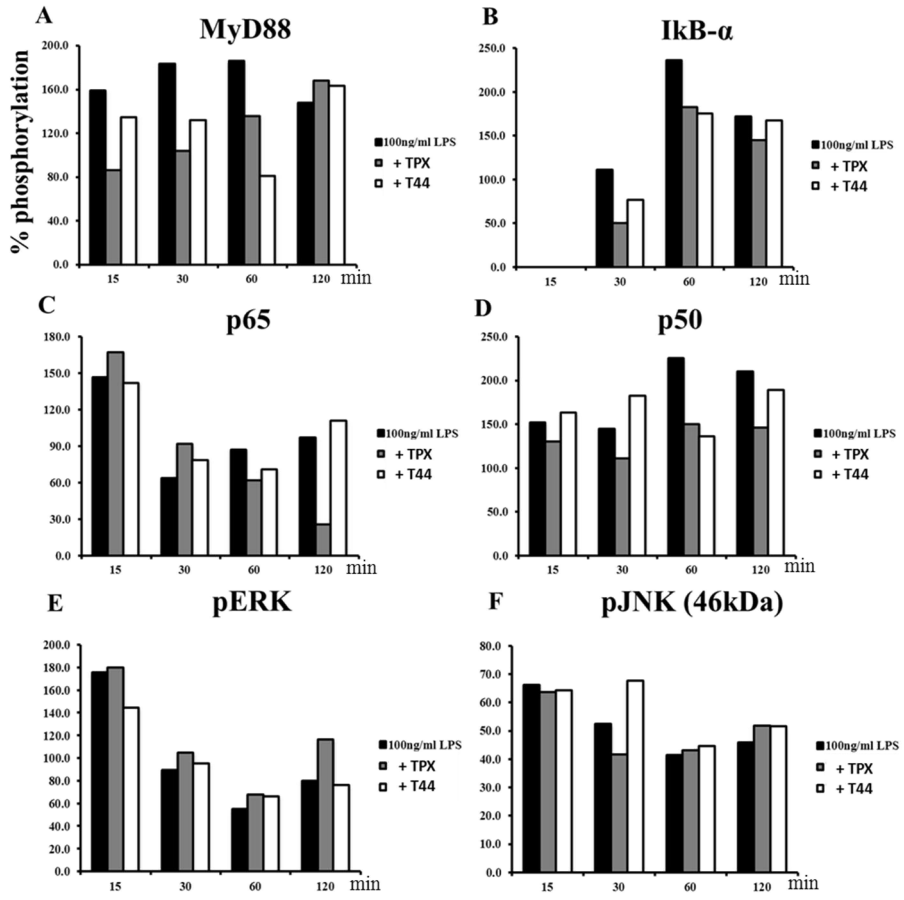

Figure 22. Diminished level of MyD88 in CS-TPX and T44 are analyzed by Image J. Data analyzed by Image J are shown as graphs normalized by actin as well as total form of each MAPKinase.

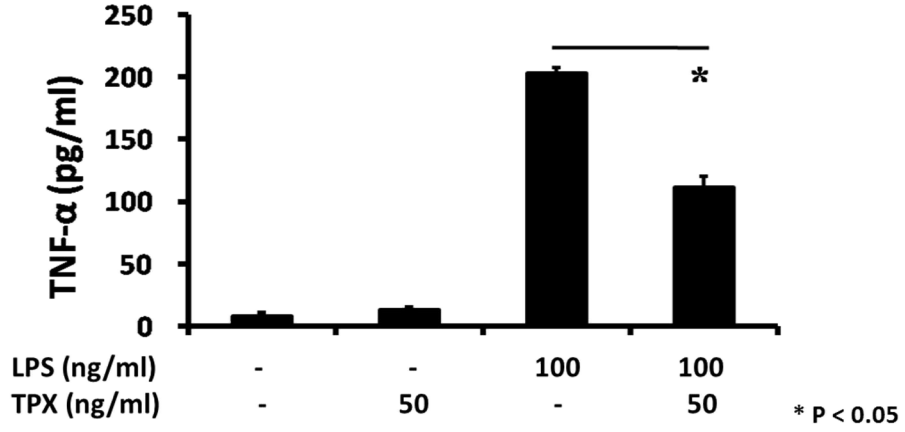

Figure 23. **CS-TPX down-regulates the LPS-induced TNF-α production from human monocyte cell line, THP-1.** Cell culture supernatants were collected after 48 h of treatment with LPS and CS-TPX. Data represent the means ± SE of three independent experiments. *$P< 0.05$ (t-test), significantly different from the value obtained in cell supernatants.

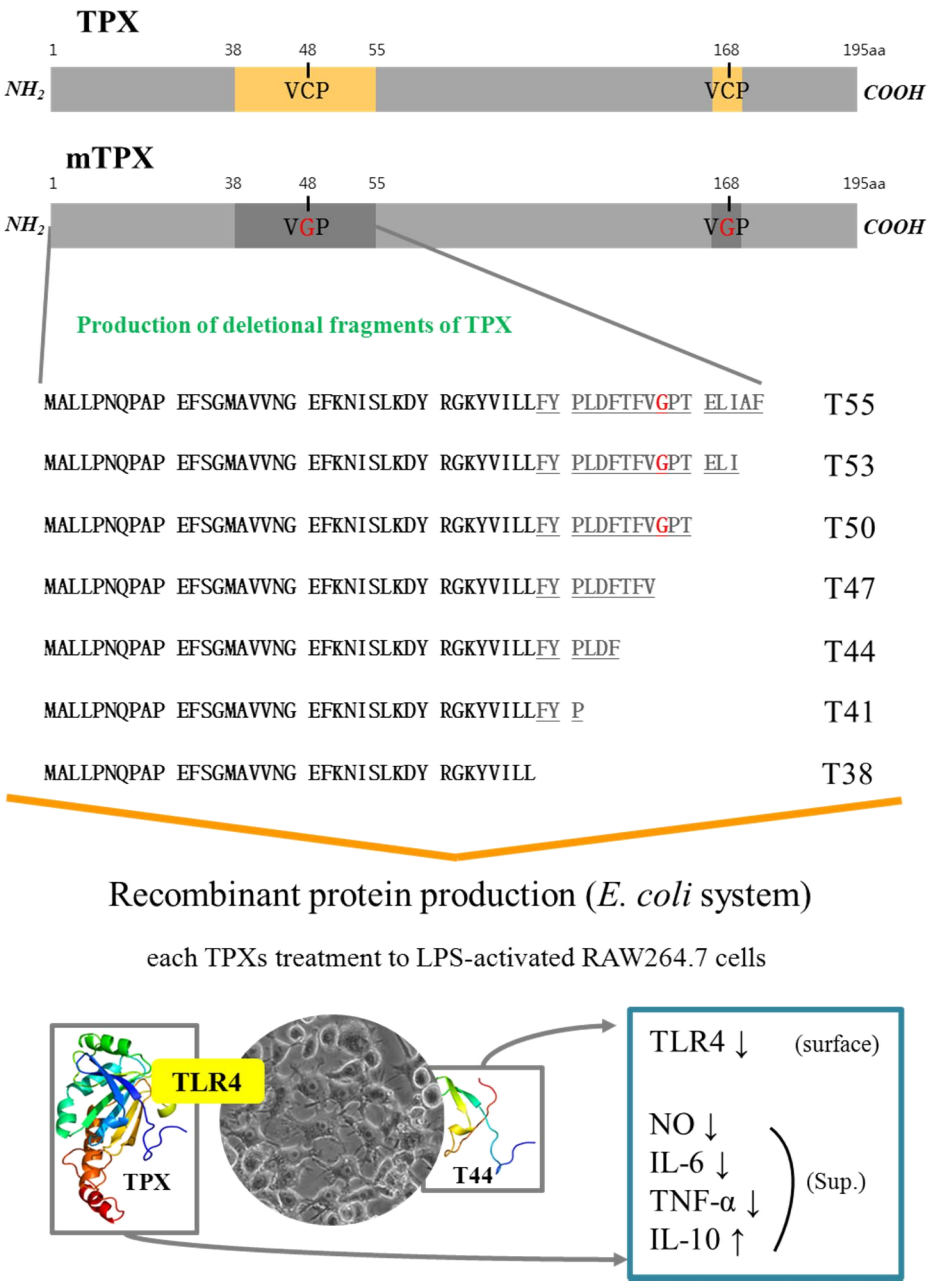

Figure 24. Summary of the dissertation

DISCUSSION

This study established new characteristics of *C. sinensis* ESP that inhibit LPS-induced production of NO and IL-6 while significantly increasing the level of IL-10 and TGF-β in RAW264.7 cells. The antigenic signal from worms to cells was initiated through the TLR4 rather than TLR2 signaling pathway, and CD86 was also increased. It may facilitate activation of cells to change their shapes into spindle-like phenotypes. Furthermore, the present result is the first description of a functional immune regulatory protein from *C. sinensis,* and the recombinant protein, CS-TPX, suppressing macrophage activation in an independent manner with enzymatic activity. Importantly, the smallest functional T44 CS-TPX was identified through a series of deletional mutants. It is not clear whether the cells of the direct worm co-culture groups have undergone cell death or not compared with indirect worm-co-culture groups (Fig. 1BE and CF). And it might be because of the physical contact between cells and eggs as well as worms crawling all around cells. Although *C. sinensis* infection generally promotes the proliferation of bile ductal epithelium (1), Fas/FasL dependent apoptosis of hepatocytes was reported in clonorchiasis (1, 71). In contrast, cells of indirect co-culture groups (Trans-worm) were well grown even in the LPS-treated condition (Fig. 1C and F). It was not surprising to discover when i referred to previous findings that *C. sinensis* ESP induce cell proliferation (10, 11); likewise, it might be due to fresh ESP, which was filtered by the transwell pore to stimulate cell proliferation of RAW264.7 cells. Interestingly, the massive production of eggs in the LPS/Trans-10 worms group than the Trans-10 worms group was observed, and i was speculate on the reason for the increased production of eggs (Fig. 1B and E). One of the purposes of the life of an organism is

production of its descendants. It would be the same for worms and the need is even stronger when they are confronted with the difficulty of survival, LPS in this experiment. That's why they make a large production of eggs since the probability of leaving their offspring is increased, in natural circumstances. Produced eggs seem to not have an additional immunomodulatory effect, as demonstrated in Figure 3 and 4 of the worm versus trans-worm groups. Since this phenomenon is observed during short periods of time (3 days), there were no dead worms but instead they showed active movement like before.

There have been many studies on the toll-receptor (TLRs) system and helminth infections (46, 72, 73). It was reported that the antigen *Opisthorchis viverrini*, which is a liver fluke like *C. sinensis*, increases the expression of TLR2 on RAW264.7 cells (74), and on peripheral blood leukocytes of opisthorchiasis patients (75). Although there is a lot of similarity in morphologic appearance, the antigenic differences would make different pathogen associated molecular patterns (PAMP); as i found in *C. sinensis*, ESP increases TLR4 but not TLR2 (Fig. 2A). It was speculated that if *C. sinensis* ESP inhibits TLR4 ligand induced inflammatory cytokines, the expression level of TLR4 would be diminished. Nevertheless, there was no reduction of the TLR4 level in LPS/worm groups but rather a slight increase in Trans/worm groups (Fig. 2C). This pattern might be related to the LPS-induced inflammatory mediators' (IL-6, NO) reduction efficacy of *C. sinensis* ESP. General TLR activation leads to the production of pro-inflammatory cytokines such as IL-6, TNF-α and type I interferon through its adaptor protein MyD88 and TRIF (76). However, in the helminth infection, it was reported that the ES-62 protein from the filarial nematode *Acanthocheilonema vitae* (*A. vitae*) inhibits macrophages, and the DC produced IL-12, TNF-α, and IL-6 levels that were induced by LPS in a TLR4 and MyD88 dependent

manner. Moreover they confirmed that the mRNA expression level of CD14 and MD-2, which is the LPS receptor complex, were increased significantly by ES-62 treatment. Instead, they assumed that ES-62 would disrupt TLR's downstream intracellular signaling to achieve its immunomodulatory effects (77). Likewise, not all TLR expression by helminth antigen induces pro-inflammatory cytokines but instead can dampen the signaling cascade according to the nature of ESP itself (72). Thus, TLR4 expression by *C. sinensis* ESP does not signify it has an initiative effect of inflammation rather it could imply the capability of interrupting crucial signaling cascades.

The regulatory role of IL-10 and TGF-B in inhibiting LPS-induced pro-inflammatory cytokines as well as NO production from monocytes has been reported (78, 79). In this study, I sought to understand how IL-10 and TGF-β produced from macrophages affect host immune responses in response to *C. sinensis* ESP; those cytokines might be in charge of the crucial role of long survival within the bile duct through the regulation of the inflammatory mediators IL-6 and NO.

It has been reported that crude antigen originated from *C. sinensis* induces ERK pathway dependent IL-10 and TGF-β production from mouse macrophages (80). And intensive production of IL-10 and TGF-β by *C. sinensis* ESP is the unique feature in this experiment. There are two possible explanations for this phenomenon. First, particular proteins within ESP activate each cytokine releasing cascade; second, ESP may have anti-inflammatory cytokine homologues. It is worth noting that studies have reported on TGF-β homologous family proteins of *H. polygyrus*, *Nippostrongylus brasiliensis* (81). Moreover, Grainger et al. examined *H. polygyrus* ESP containing TGF-b-like activity, and 10ug/ml of ESP represents a comparable effect with 0.5-5ng/ml of recombinant human TGF-β1 (37).

Because there was no synergistic production of IL-10 and TGF-β in LPS treatment groups in contrast to normal worm co-culture groups, it was presumed that *C. sinensis* ESP may possess TGF-β homologues.

Studies on helminth infection narrow down its focus to a functional molecule that has specific regulatory properties enabling it to be developed into therapeutic medicine for use in allergy and autoimmune diseases (82). The specific antigen B (AgB) from *Echinococcus granulosus* reduces human DC expressed co-stimulatory molecules and induces Th2 responses (83). AvCystatin from *A. vitae* has an effect on the downregulation of T cell responses and promotes the induction of IL-10 from macrophages (84, 85). PAS-1 from *Ascaris suum* (*A. suum*) inhibits pro-inflammatory cytokine and induces IL-10 and TGF-β (86).

Once *C. sinensis* infects humans, the worms can survive within the bile duct for significant periods, potentially more than 10 years (1). However, it has not been clarified how *C. sinensis* lives for such long periods. Here i demonstrated that the macrophage regulating property of *C. sinensis* ESP has increased production of anti-inflammatory cytokines but decreased production of the LPS-induced pro-inflammatory mediator, which may be in charge of one of the mechanisms.

The gene expression profile of adult *C. sinensis* was reported through analyzing expressed sequence tags (ESTs) and 12,830 EST sequences were assembled (87). According to the data, cysteine proteases, cysteine protease inhibitor and antioxidant enzymes were relatively more abundant in adults than in the egg and metacercaria stages. These expressions may be essential for successful establishment of parasitism because they play a crucial role in evasion from host immune responses, protection from digestive protease and regulation of host-induced ROS production (87).

Peroxiredoxin exploits cysteine sulfur atoms to reduce H_2O_2 and organic peroxides. It was originally divided into two classes, which is 1-Cys and 2-Cys peroxiredoxin, based on the number of cysteinyl residues; and in the case of 2-Cys peroxiredoxin, called TPX, identified by the conservation of the two redox-active cysteines (61). Wood et al (2003) well documented the character of peroxiredoxin and summarized the steps of TPX reaction. The first step is the action of peroxidatic cysteine (generally near residue 50 aa) which is conserved at 48 aa of CS-TPX. Following the peroxidase reaction is the resolution of the cysteine sulfenic acid acting as resolving cysteine (generally near residue 170 aa), which is conserved at 169 aa of TPX (88).

Although TPX is further divided into two subtypes, which is 'typical' and 'atypical' by the site of resolving cysteine within the polypeptide, they are functionally equivalent. As shown in Fig 6, because CS-TPX has two cysteine residues at different amino acid sites, it represents TPX as typical 2-Cys peroxiredoxin. Moreover, there was none of the available atypical 2-Cys peroxiredoxin in helminth ESTs and/or the genome data (89).

The expression pattern of TPX within *C. sinensis* antigens has shown that it is a not only conserved in the whole worm as well as the germ cell itself but also secreted to the extra-environment (Fig. 5D). Moreover, IHC results on the distribution of TPX in *C. sinensis* infected liver tissue support this hypothesis. It is conserved in the worm body (tegument, seminal receptacle, intestine and eggs) and its impact on the hepatic epithelial cells may be to neutralize the harmful ROS (Fig. 8). However, the SignalIP result lets us know that CS-TPX does not contain predictable N-terminal signal peptide, which directs the transport of protein to ER/Golgi for secretion. Robin et al. (2009) hypothesized that *F. hepatica* peroxiredoxin and other antioxidant proteins that lack signal peptide can be secreted via the ATP-binding cassette

(ABC) protein transporter and phospholipase into plasma membrane micro-vesicles (90). Therefore, these findings support that CS-TPX can be secreted via non-classical secretory pathways of *C. sinensis*.

The TLR4 down-regulatory effect of CS-TPX and LPS co-culture groups was observed and it could be because of direct binding of CS-TPX to TLR4. In the case of LPS, however, they do not bind to TLR4 directly but interact with MD-2 through CD14 so that make LPS-MD-2-TLR4 complex (91). The possibility of TPX binding to TLR4 directly was already examined by recombinant human peroxiredoxin I, and the results show that the interaction of peroxiredoxin with TLR4 occurred in a CD14, MD2 dependent manner. This interaction causes endocytosis of TLR4 and induces proinflammatory cytokine secretion from macrophage cells. Interestingly, this interaction between peroxiredoxin and TLR4 independent of its peroxidase property but dependent on its chaperone property was elucidated (92). Although, the direct interaction outcome of TPX and peroxiredoxin with TLR4 differed, the possibility of structural or sequence basis crosstalk would be identical. In the case of helminth produced molecules, it was reported that ES-62 protein blocks LPS-triggered inflammatory signaling via autophagosome-mediated downregulation of the TLR4 and MyD88. Furthermore, this downregulation of macrophage activation was also demonstrated to lead to the protection of mice from endotoxin shock (93). Thus, these findings show that the CS-TPX inhibits LPS-induced TLR4 expression through direct interaction could be possible.

The function of TPX as a negative regulator for LPS-induced activation of macrophages is a striking feature of CS-TPX. It is reported that the production of LPS-induced ROS and proinflammatory mediators surged in endogenous TPX knockout cells compared with TPX overexpressed cells (67). This result

showed that TPX may be engaged in an LPS-activated signaling cascade and MAPKinases, NF-κB would be the primary considerations. The results demonstrated that TPX regulates MAPKinase p-p38, p-ERK and p-IKKα/IKKβ. Furthermore, it was confirmed that sensitivity to LPS-induced lethal shock was enhanced in TPX deficient mice. This finding supports the idea that CS-TPX had anti-inflammatory properties and a role in the reduction of proinflammatory cytokine, which could be involved in the MAPKinase of NF-κB. However, the immunoblotting results show expression levels of MAPK as well as NF-κB heterodimers, p-65 and p50 were not affected by CS-TPX and T44 treatment (Fig. 21 – 22). A greater decrease in the expression profile of the MyD88 level was observed in the CS-TPXs (15 – 60 min) than in the LPS treatment groups (Fig. 21 – 22A). These discrepancies might come from an existing and active site of each peroxiredoxin and CS-TPXs, because the latter acts through the extracellular region of the TLR4 rather than cytoplasm. Future studies need to identify adaptor molecules that are affected and regulated by CS-TPXs.

TLR4 is the most unique receptor among all TLRs because its ability to activate two distinct signaling pathways. It recruits MyD88 by sorting the receptor TIRAP (Toll/interleukin-1-receptor (TIR)-domain-containing adaptor protein) and also recruits TRAM through the adaptor protein TRIF (TIR-domain containing adaptor protein inducing interferon-β). These two signaling pathways take place sequentially at different locations of the cellular component. During the initial TLR4 signaling, the LPS-CD14-MD2-TLR4 complex preferentially binds with TIRAP-MyD88 at the plasma membrane so to trigger induction of pro-inflammatory cytokines. These receptor complexes were endocytosed to early endosome and loss of TIRAP-MyD88 complex within endosome allows the TRAM-TRIF complex to trigger induction of

type I interferons (94). The transcription factors participate in TLR4 induced target gene expression by cooperating with E2F1 or controlling their expression through C/EBP and JMJD3 (95). Inducing genes were categorized into three subsets by the order of expression. Tnf, Ptgs2 and Nfkbia genes are expressed the most rapidly and then Ccl5 and Ccl2, so as to categorize early and late primary genes, respectively. In contrast, because they often require SW1/SNF-dependent nucleosomal remodeling of Nos, Il12b and Il6 are considered as secondary response genes. Furthermore, it was reported that NFAT5, which is originally considered as an osmo-stress responsive factor, recruited and bound to *Nos2* promoter in the circumstance of LPS stimulated macrophages to regulate TLR-induced iNOS expression (96). Likewise, further study will be required to address whether TLR4 triggered plasma membrane TIRAP-MyD88 signaling and early endosomal TRIF-TRAM signaling induced target gene expression profiles are regulated by CS-TPXs or not.

It is reported that recombinant TPX of *F. hepatica* promotes alternatively activated macrophages, which is a specific macrophage subtype in some helminth infections, and through this mechanism TPX from *F. hepatica* and *S. mansoni* direct the T cell response toward parasite specific T_H2 responses (50, 51, 97). It is interesting that the immunogenic property of TPX is not related with its enzymatic activity (51, 92). Therefore, the detailed mechanism of the novel function of CS-TPX was further investigated to minimize the functional amino acid of CS-TPX. The smallest CS-TPX, which has functional properties, was T44 and the sequential difference between T44 and T41 was 41/LDF amino acids (Fig. 15). The predicted structural difference between T44 and 41 was ignorable (Fig. 20) and the efficacy of the down-modulatory effect on TLR4, NO, IL-6 and TNF-α was comparable to that of CS-TPX and

T44 but not T41. The results implied CS-TPX functional activity could be delivered through its sequential basis mechanism.

Relatively low levels of IL-10 production (ESP: up to 4ng/ml, TPX: up to 70pg/ml) were observed (Fig. 4A, Fig. 10D). This phenomenon might be because of differences in culture periods (3 days with ESP and 18hrs with TPX) and more cytokines would be produced as time goes by. Undetectable TGF-β secretion from CS-TPX conditioned RAW264.7 cells is also a striking difference compared wtih *C. sinensis* ESP, as shown in Fig.4B. It is assumed that *C. sinensis* ESP is composed of a considerable complex of proteins and carbohydrates but CS-TPX is a single protein. That's why the property of CS-TPX was simpler in LPS-induced activation of RAW264.7 cells than ESP.

Although it has not clarified all aspects of CS-ESP and CS-TPX induced immune regulatory property yet, CS-TPX, especially the smallest T44, is in charge of a part for negative regulator in LPS treated macrophages, and it would be the crucial mechanism to establishing long-term survival in a harmful environment, bile ducts.

The specific helminth-derived product development seems to be beneficial because it permits the guarantee of safety and stability in a product that can be produced without the need of an intermediate animal host (e.g., porcine for *T. suis* ova). Furthermore, it is advantageous to evade the host immune reaction when it is administrated into the host as the smallest amino acid sequence representing the smallest foreign-protein to the host. Since thioredoxin, an electron donor of TPX, is highly regarded as an immunosuppressant for acute inflammatory disorder, CS-T44 will be a future focus of developmental therapeutics.

REFERENCES

1. Hong ST. *Clonorchis sinensis*. In: Miliotis MD BJ, editor. International handbook of foodborne pathogens. Marcel Dekker: New York; 2003. p. 581-92.
2. Kim TS, Cho SH, Huh S, Kong Y, Sohn WM, Hwang SS, et al. A Nationwide Survey on the Prevalence of Intestinal Parasitic Infections in the Republic of Korea, 2004. Korean J Parasitol. 2009;47(1):37-47.
3. Hong ST, Fang YY. *Clonorchis sinensis* and clonorchiasis, an update. Parasitol Int. 2012;61(1):17-24.
4. Schwartz DA. Helminths in the induction of cancer: *Opisthorchis viverrini*, *Clonorchis sinensis* and cholangiocarcinoma. Trop Geogr Med. 1980;32:95-100.
5. Watanapa P, Watanapa WB. Liver fluke-associated cholangiocarcinoma. Br J Surg. 2002;89(8):962-70.
6. Choi D, Lim JH, Lee KT, Lee JK, Choi SH, Heo JS, et al. Cholangiocarcinoma and *Clonorchis sinensis* infection: a case-control study in Korea. J Hepatol. 2006;44(6):1066-73.
7. Lee JH, Rim HJ, Bak UB. Effect of *Clonorchis sinensis* infection and dimethylnitrosamine administration on the induction of cholangiocarcinoma in Syrian golden hamsters. Korean J Parasitol. 1993;31(1):21-30.
8. Lim MK, Ju YH, Franceschi S, Oh JK, Kong HJ, Hwang SS, et al. *Clonorchis sinensis* infection and increasing risk of cholangiocarcinoma in the Republic of Korea. Am J Trop Med Hyg. 2006;75(1):93-6.
9. Suarez-Munoz MA, Fernandez-Aguilar JL, Sanchez-Perez B, Perez-Daga JA, Garcia-Albiach B, Pulido-Roa Y, et al. Risk factors and classifications of hilar cholangiocarcinoma. World J Gastrointest Oncol. 2013;5(7):132-8.
10. Kim YJ, Choi MH, Hong ST, Bae YM. Resistance of

cholangiocarcinoma cells to parthenolide-induced apoptosis by the excretory-secretory products of *Clonorchis sinensis*. Parasitol Res. 2009;104(5):1011-6.

11. Kim YJ, Choi MH, Hong ST, Bae YM. Proliferative effects of excretory/secretory products from *Clonorchis sinensis* on the human epithelial cell line HEK293 via regulation of the transcription factor E2F1. Parasitol Res. 2008;102(3):411-7.
12. Pak J, Kim DW, Moon J, Nam JH, Kim JH, Ju JW, et al. Differential gene expression profiling in human cholangiocarcinoma cells treated with *Clonorchis sinensis* excretory-secretory products. Parasitol Res. 2009;104(5):1035-46.
13. Kim DW, Kim JY, Moon JH, Kim KB, Kim TS, Hong SJ, et al. Transcriptional induction of minichromosome maintenance protein 7 (Mcm7) in human cholangiocarcinoma cells treated with *Clonorchis sinensis* excretory-secretory products. Mol Biochem Parasitol. 2010;173(1):10-6.
14. Lee JH, Rim HJ, Bak UB. Effect of *Clonorchis sinensis* infection and dimethylnitrosamine administration on the induction of cholangiocarcinoma in Syrian golden hamsters. Korean J Parasitol. 1993;31(1):21-30.
15. Choi YK, Yoon BI, Won YS, Lee CH, Hyun BH, Kim HC, et al. Cytokine responses in mice infected with *Clonorchis sinensis*. Parasitol Res. 2003;91(2):87-93.
16. Yoon BI, Choi YK, Kim DY, Hyun BH, Joo KH, Rim HJ, et al. Infectivity and pathological changes in murine clonorchiasis: Comparison in immunocompetent and immunodeficient mice. J Vet Med Sci. 2001;63(4):421-5.
17. Crispe IN. The Liver as a Lymphoid Organ. Annu Rev Immunol. 2009;27:147-63.
18. Fallon PG, Mangan NE. Suppression of TH2-type allergic reactions by helminth infection. Nat Rev Immunol. 2007;7(3):220-30.
19. Atochina O, Daly-Engel T, Piskorska D, McGuire E, Harn DA. A

schistosome-expressed immunomodulatory glycoconjugate expands peritoneal Gr1(+) macrophages that suppress naive CD4(+) T cell proliferation via an IFN-gamma and nitric oxide-dependent mechanism. J Immunol. 2001;167(8):4293-302.

20. Smith P, Walsh CM, Mangan NE, Fallon RE, Sayers JR, McKenzie ANJ, et al. *Schistosoma mansoni* worms induce anergy of T cells via selective up-regulation of programmed death ligand 1 on macrophages. J Immunol. 2004;173(2):1240-8.
21. Maizels RM, Yazdanbakhsh M. Immune regulation by helminth parasites: Cellular and molecular mechanisms. Nat Rev Immunol. 2003;3(9):733-44.
22. Satoguina JS, Adjobimey T, Arndts K, Hoch J, Oldenburg J, Layland LE, et al. Tr1 and naturally occurring regulatory T cells induce IgG4 in B cells through GITR/GITR-L interaction, IL-10 and TGF-beta. Eur J Immunol. 2008;38(11):3101-13.
23. White RR, Artavanis-Tsakonas K. How helminths use excretory secretory fractions to modulate dendritic cells. Virulence. 2012;3(7):668-77.
24. Taylor MD, Harris A, Nair MG, Maizels RM, Allen JE. F4/80+ alternatively activated macrophages control CD4+ T cell hyporesponsiveness at sites peripheral to filarial infection. J Immunol. 2006;176(11):6918-27.
25. Nair MG, Gallagher LJ, Taylor MD, Loke P, Coulson PS, Wilson RA, et al. Chitinase and Fizz family members are a generalized feature of nematode infection with selective Upregulation of Ym1 and F10.1 by antigen-presenting cells. Infect Immun. 2005;73(1):385-94.
26. Chen F, Liu ZG, Wu WH, Rozo C, Bowdridge S, Millman A, et al. An essential role for TH2-type responses in limiting acute tissue damage during experimental helminth infection. Nat Med. 2012;18(2):260-6.
27. Wilson MS, Taylor MD, Balic A, Finney CAM, Lamb JR, Maizels RM. Suppression of allergic airway inflammation by helminth-induced regulatory T cells. J Exp Med. 2005;202(9):1199-212.

28. van den Biggelaar AHJ, van Ree R, Rodrigues LC, Lell B, Deelder AM, Kremsner PG, et al. Decreased atopy in children infected with *Schistosoma haematobium*: a role for parasite-induced interleukin-10. Lancet. 2000;356(9243):1723-7.
29. Fleming JO. Helminth therapy and multiple sclerosis. Int J Parasitol. 2013;43(3-4):259-74.
30. Sartono E, Kruize YCM, Kurniawan A, Vandermeide PH, Partono F, Maizels RM, et al. Elevated cellular immune responses and interferon-gamma release after long-term diethylcarbamazine treatment of patients with human lymphatic filariasis. J Infect Dis. 1995;171(6):1683-7.
31. Semnani RT, Law M, Kubofcik J, Nutman TB. Filaria-induced immune evasion: Suppression by the infective stage of *Brugia malayi* at the earliest host-parasite interface. J Immunol. 2004;172(10):6229-38.
32. Lightowlers MW, Rickard MD. Excretory-secretory products of helminth parasites: effects on host immune responses. Parasitology. 1988;96:S123-S66.
33. Hewitson JP, Grainger JR, Maizels RM. Helminth immunoregulation: the role of parasite secreted proteins in modulating host immunity. Mol Biochem Parasitol. 2009;167(1):1-11.
34. Falcon C, Carranza F, Martinez FF, Knubel CP, Masih DT, Motran CC, et al. Excretory-secretory products (ESP) from Fasciola hepatica induce tolerogenic properties in myeloid dendritic cells. Vet Immunol Immunop. 2010;137(1-2):36-46.
35. Jenkins SJ, Mountford AP. Dendritic cells activated with products released by schistosome larvae drive Th2-type immune responses, which can be inhibited by manipulation of CD40 costimulation. Infect Immun. 2005;73(1):395-402.
36. Everts B, Hussaarts L, Driessen NN, Meevissen MHJ, Schramm G, van der Ham AJ, et al. Schistosome-derived omega-1 drives Th2 polarization by suppressing protein synthesis following internalization by the mannose receptor. J Exp Med. 2012;209(10):1753-67.
37. Grainger JR, Smith KA, Hewitson JP, McSorley HJ, Harcus Y, Filbey KJ,

et al. Helminth secretions induce de novo T cell Foxp3 expression and regulatory function through the TGF-beta pathway. J Exp Med. 2010;207(11):2331-41.

38. Meyer S, van Liempt E, Imberty A, van Kooyk Y, Geyer H, Geyer R, et al. DC-SIGN mediates binding of dendritic cells to authentic pseudo-LewisY glycolipids of *Schistosoma mansoni* cercariae, the first parasite-specific ligand of DC-SIGN. J Biol Chem. 2005;280(45):37349-59.
39. van Liempt E, van Vliet SJ, Engering A, Vallejo JJG, Bank CMC, Sanchez-Hernandez M, et al. *Schistosoma mansoni* soluble egg antigens are internalized by human dendritic cells through multiple C-type lectins and suppress TLR-induced dendritic cell activation. Mol Immunol. 2007;44(10):2605-15.
40. van Die I, Cummings RD. Glycan gimmickry by parasitic helminths: a strategy for modulating the host immune response? Glycobiology. 2010;20(1):2-12.
41. McInnes IB, Gracie JA, Leung BP, Harnett M, Liew FY, Harnett W. A novel therapeutic approach targeting articular inflammation using the filarial nematode derived phosphoryleholine-containing glycoprotein, ES-62. J Immunol. 2003;171(4):2127-33.
42. Melendez AJ, Harnett MM, Pushparaj PN, Wong WF, Tay HK, McSharry CP, et al. Inhibition of Fc epsilon RI-mediated mast cell responses by ES-62, a product of parasitic filarial nematodes. Nat Med. 2007;13(11):1375-81.
43. Everts B, Perona-Wright G, Smits HH, Hokke CH, van der Ham AJ, Fitzsimmons CM, et al. Omega-1, a glycoprotein secreted by *Schistosoma mansoni* eggs, drives Th2 responses. J Exp Med. 2009;206(8):1673-80.
44. van der Kleij D, Latz E, Brouwers JFHM, Kruize YCM, Schmitz M, Kurt-Jones EA, et al. A novel host-parasite lipid cross-talk. Schistosomal lyso-phosphatidylserine activates toll-like receptor 2 and affects immune polarization. J Biol Chem. 2002;277(50):48122-9.
45. Harn DA, McDonald J, Atochina O, Da'dara AA. Modulation of host

immune responses by helminth glycans. Immunol Rev. 2009;230:247-57.

46. Donnelly S, O'Neill SM, Stack CM, Robinson MW, Turnbull L, Whitchurch C, et al. Helminth cysteine proteases inhibit TRIF-dependent activation of macrophages via degradation of TLR3. J Biol Chem. 2010;285(5):3383-92.
47. Doetze A, Satoguina J, Burchard G, Rau T, Loliger C, Fleischer B, et al. Antigen-specific cellular hyporesponsiveness in a chronic human helminth infection is mediated by T(h)3/T(r)1-type cytokines IL-10 and transforming growth factor-beta but not by a T(h)1 to T(h)2 shift. Int Immunol. 2000;12(5):623-30.
48. Schnoeller C, Rausch S, Pillai S, Avagyan A, Wittig BM, Loddenkemper C, et al. A helminth immunomodulator reduces allergic and inflammatory responses by induction of IL-10-producing macrophages. J Immunol. 2008;180(6):4265-72.
49. Rzepecka J, Rausch S, Klotz C, Schnoller C, Kornprobst T, Hagen J, et al. Calreticulin from the intestinal nematode *Heligmosomoides polygyrus* is a Th2-skewing protein and interacts with murine scavenger receptor-A. Mol Immunol. 2009;46(6):1109-19.
50. Donnelly S, O'Neill SM, Sekiya M, Mulcahy G, Dalton JP. Thioredoxin peroxidase secreted by *Fasciola hepatica* induces the alternative activation of macrophages. Infect Immun. 2005;73(1):166-73.
51. Donnelly S, Stack CM, O'Neill SM, Sayed AA, Williams DL, Dalton JP. Helminth 2-Cys peroxiredoxin drives Th2 responses through a mechanism involving alternatively activated macrophages. FASEB J. 2008;22(11):4022-32.
52. Callahan HL, Crouch RK, James ER. Helminth Anti-Oxidant Enzymes - a Protective Mechanism against Host Oxidants. Parasitol Today. 1988;4(8):218-25.
53. Chiumiento L, Bruschi F. Enzymatic antioxidant systems in helminth parasites. Parasitol Res. 2009;105(3):593-603.
54. Rhee SG, Chae HZ, Kim K. Peroxiredoxins: A historical overview and speculative preview of novel mechanisms and emerging concepts in cell

signaling. Free Radic Biol Med. 2005;38(12):1543-52.

55. Mates JM. Effects of antioxidant enzymes in the molecular control of reactive oxygen species toxicology. Toxicology. 2001;163(2-3):219-.
56. Mei HP, LoVerde PT. Schistosoma mansoni: The developmental regulation and immunolocalization of antioxidant enzymes. Exp Parasitol. 1997;86(1):69-78.
57. Selkirk ME, Smith VP, Thomas GR, Gounaris K. Resistance of filarial nematode parasites to oxidative stress. Int J Parasitol. 1998;28(9):1315-32.
58. McGonigle S, Curley GP, Dalton JP. Cloning of peroxiredoxin, a novel antioxidant enzyme, from the helminth parasite *Fasciola hepatica*. Parasitology. 1997;115:101-4.
59. Kwatia MA, Botkin DJ, Williams DL. Molecular and enzymatic characterization of *Schistosoma mansoni* thioredoxin peroxidase. J Parasitol. 2000;86(5):908-15.
60. Tsuji N, Kasuga-Aoki H, Isobe T, Yoshihara S. Cloning and characterisation of a peroxiredoxin from the swine roundworm *Ascaris suum*. Int J Parasitol. 2000;30(2):125-8.
61. Chae HZ, Chung SJ, Rhee SG. Thioredoxin-Dependent Peroxide Reductase from Yeast. J Biol Chem. 1994;269(44):27670-8.
62. Fourquet S, Huang ME, D'Autreaux B, Toledano MB. The dual functions of thiol-based peroxidases in H2O2 scavenging and signaling. Antioxid Redox Sign. 2008;10(9):1565-75.
63. Fujii J, Ikeda Y. Advances in our understanding of peroxiredoxin, a multifunctional, mammalian redox protein. Redox Rep. 2002;7(3):123-30.
64. Kim H, Lee TH, Park ES, Suh JM, Park SJ, Chung HK, et al. Role of peroxiredoxins in regulating intracellular hydrogen peroxide and hydrogen peroxide-induced apoptosis in thyroid cells. J Biol Chem. 2000;275(24):18266-70.
65. Wen ST, VanEtten RA. The PAG gene product, a stress-induced protein with antioxidant properties, is an Abl SH3-binding protein and a

physiological inhibitor of c-Abl tyrosine kinase activity. Genes & development. 1997;11(19):2456-67.

66. Moon EY, Noh YW, Han YH, Kim SU, Kim JM, Yu DY, et al. T lymphocytes and dendritic cells are activated by the deletion of peroxiredoxin II (Prx II) gene. Immunol Lett. 2006;102(2):184-90.
67. Yang CS, Lee DS, Song CH, An SJ, Li SJ, Kim JM, et al. Roles of peroxiredoxin II in the regulation of proinflammatory responses to LPS and protection against endotoxin-induced lethal shock. J Exp Med. 2007;204(3):583-94.
68. Misko TS, R.; Salvemini, D.; Moore, W.; Currie, M. AFluorometric assay for the measurement of nitrite in biological samples. Anal Biochem. 1993(214):11-6.
69. Kelley LA, Sternberg MJE. Protein structure prediction on the Web: a case study using the Phyre server. Nat Protoc. 2009;4(3):363-71.
70. Arnold K, Bordoli L, Kopp J, Schwede T. The SWISS-MODEL workspace: a web-based environment for protein structure homology modelling. Bioinformatics. 2006;22(2):195-201.
71. Zhang XL, Jin ZF, Da R, Dong YX, Song WQ, Chen XB, et al. Fas/FasL-dependent apoptosis of hepatocytes induced in rat and patients with *Clonorchis sinensis* infection. Parasitol Res. 2008;103(2):393-9.
72. Venugopal PG, Nutman TB, Semnani RT. Activation and regulation of toll-like receptors (TLRs) by helminth parasites. Immunol Res. 2009;43(1-3):252-63.
73. Jenkins SJ, Hewitson JP, Ferret-Bernard S, Mountford AP. Schistosome larvae stimulate macrophage cytokine production through TLR4-dependent and -independent pathways. Int Immunol. 2005;17(11):1409-18.
74. Pinlaor S, Tada-Oikawa S, Hiraku Y, Pinlaor P, Ma N, Sithithaworn P, et al. *Opisthorchis viverrini* antigen induces the expression of Toll-like receptor 2 in macrophage RAW cell line. Int J Parasitol. 2005;35(6):591-6.
75. Yongvanit P, Thanan R, Pinlaor S, Sithithaworn P, Loilome W, Namwat

N, et al. Increased expression of TLR-2, COX-2, and SOD-2 genes in the peripheral blood leukocytes of opisthorchiasis patients induced by *Opisthorchis viverrini* antigen. Parasitol Res. 2012;110(5):1969-77.

76. Kawai T, Akira S. The role of pattern-recognition receptors in innate immunity: update on Toll-like receptors. Nat Immunol. 2010;11(5):373-84.
77. Goodridge HS, Marshall FA, Else KJ, Houston KM, Egan C, Al-Riyami L, et al. Immunomodulation via novel use of TLR4 by the filarial nematode phosphorylcholine-containing secreted product, ES-62. J Immunol. 2005;174(1):284-93.
78. Malefyt RD, Abrams J, Bennett B, Figdor CG, Devries JE. Interleukin-10(Il-10) Inhibits Cytokine Synthesis by Human Monocytes - an Autoregulatory Role of Il-10 Produced by Monocytes. J Exp Med. 1991;174(5):1209-20.
79. Zissel G, Schlaak J, Schlaak M, MullerQuernheim J. Regulation of cytokine release by alveolar macrophages treated with interleukin-4, interleukin-10, or transforming growth factor beta. Eur Cytokine Netw. 1996;7(1):59-66.
80. Wi HJ, Jin Y, Choi MH, Hong ST, Bae YM. Predominance of IL-10 and TGF-beta production from the mouse macrophage cell line, RAW264.7, in response to crude antigens from *Clonorchis sinensis*. Cytokine. 2012;59(2):237-44.
81. McSorley HJ, Grainger JR, Harcus Y, Murray J, Nisbet AJ, Knox DP, et al. daf-7-related TGF-beta homologues from Trichostrongyloid nematodes show contrasting life-cycle expression patterns. Parasitology. 2010;137(1):159-71.
82. Johnston MJG, MacDonald JA, Mckay DM. Parasitic helminths : a pharmacopeia of anti-inflammatory molecules. Parasitology. 2009;136(2):125-47.
83. Rigano R, Buttari B, Profumo E, Ortona E, Delunardo F, Margutti P, et al. *Echinococcus granulosus* antigen B impairs human dendritic cell differentiation and polarizes immature dendritic cell maturation towards

a Th2 cell response. Infect Immun. 2007;75(4):1667-78.

84. Klotz C, Ziegler T, Figueiredo AS, Rausch S, Hepworth MR, Obsivac N, et al. A helminth immunomodulator exploits host signaling events to regulate cytokine production in macrophages. PLoS pathogens. 2011;7(1).
85. Hartmann S, Kyewski B, Sonnenburg B, Lucius R. A filarial cysteine protease inhibitor downregulates T cell proliferation and enhances interleukin-10 production. Eur J Immunol. 1997;27(9):2253-60.
86. Oshiro TM, Macedo MS, Macedo-Soares MF. Anti-inflammatory activity of PAS-1, a protein component of *Ascaris suum*. Inflamm Res. 2005;54(1):17-21.
87. Yoo WG, Kim DW, Ju JW, Cho PY, Kim TI, Cho SH, et al. Developmental Transcriptomic Features of the Carcinogenic Liver Fluke, *Clonorchis sinensis*. PLoS Negl Trop Dis. 2011;5(6).
88. Wood ZA, Schroder E, Harris JR, Poole LB. Structure, mechanism and regulation of peroxiredoxins. Trends Biochem Sci. 2003;28(1):32-40.
89. Robinson MW, Hutchinson AT, Dalton JP, Donnelly S. Peroxiredoxin: a central player in immune modulation. Parasite Immunol. 2010;32(5):305-13.
90. Robinson MW, Menon R, Donnelly SM, Dalton JP, Ranganathan S. An integrated transcriptomics and proteomics analysis of the secretome of the helminth pathogen *Fasciola hepatica*: proteins associated with invasion and infection of the mammalian host. Mol Cell Proteomics. 2009;8(8):1891-907.
91. Akashi S, Saitoh S, Wakabayashi Y, Kikuchi T, Takamura N, Nagai Y, et al. Lipopolysaccharide interaction with cell surface toll-like receptor 4-MD-2: Higher affinity than that with MD-2 or CD14. J Exp Med. 2003;198(7):1035-42.
92. Riddell JR, Wang XY, Minderman H, Gollnick SO. Peroxiredoxin 1 Stimulates Secretion of Proinflammatory Cytokines by Binding to TLR4. J Immunol. 2010;184(2):1022-30.
93. Puneet P, McGrath MA, Tay HK, Al-Riyami L, Rzepecka J, Moochhala SM, et al. The helminth product ES-62 protects against septic shock via

Toll-like receptor 4-dependent autophagosomal degradation of the adaptor MyD88 (Retracted article. See vol. 12, pg. 804, 2011). Nat Immunol. 2011;12(4):344-U100.

94. Kagan JC, Su T, Horng T, Chow A, Akira S, Medzhitov R. TRAM couples endocytosis of Toll-like receptor 4 to the induction of interferon-beta. Nat Immunol. 2008;9(4):361-8.
95. Takeuchi O, Akira S. Pattern Recognition Receptors and Inflammation. Cell. 2010;140(6):805-20.
96. Buxade M, Lunazzi G, Minguillon J, Iborra S, Berga-Bolanos R, del Val M, et al. Gene expression induced by Toll-like receptors in macrophages requires the transcription factor NFAT5. J Exp Med. 2012;209(2):379-93.
97. Kreider T, Anthony RM, Urban JF, Gause WC. Alternatively activated macrophages in helminth infections. Curr Opin Immunol. 2007;19(4):448-53.

국문 초록

간흡충은 숙주의 담관내에 기생하며 무증상으로 만성 감염한다. 기생충 감염에 따른 숙주 면역 반응의 저하는 살아있는 충체에서 분비된 분비배설항원에서 기인하는 것으로 알려져 있다. 간흡충의 만성감염 기전을 규명하고자 살아있는 간흡충의 성충과 마우스의 대식세포주인 RAW264.7 세포와 투과성 transwll 을 이용해 공동배양 했을 때, 세포 표면의 TLR4 발현증가가 관찰되었고 LPS 에 의한 염증 매개물질인 IL-6 와 NO 의 감소가 관찰되었다. 반면, 항 염증성 매개물질인 IL-10 과 TGF-β의 분비 증가가 관찰되었다. 기존에 보고된 논문들을 바탕으로 조사한 결과 기생연충의 분비배설항원 내에 존재하는 항산화 효소인 TPX 는 대식세포를 매개로 하여 숙주의 면역반응을 Th2 쪽으로 치우치게 하는 기능을 내포하고 있음을 알 수 있었다. 간흡충의 분비배설항원 내 면역조절을 담당하는 후보 단백질을 TPX 로 선정하고 최초로 클로닝을 시도하였다. 실험을 통해 밝혀진 DNA/protein 시퀀스를 Genbank 에 등록했다 (AND65138.1). 또한 *E. coli* 시스템을 이용하여 재조합 단백질을 생산하여 RAW264.7 세포에 처리했을 때 LPS 에 의해 증가된 TLR4 발현 감소와 더불어 NO, IL-6 및 TNF-α의 세포 배양액 내 발현 감소가 관찰되었다. 반대로 항염증성 사이토카인인 IL-10 의 생산 증가가 관찰되었으나 TGF-β는 분비되지 않았다. GST fusion 단백질을 이용한 Pull-down assay 결과 TPX 가 TLR4 와 직접적으로 상호작용함이 관찰되었다. 여러 가지의 작은 TPX 를 만들어 동일한 실험을 진행한 결과 T44

TPX 가 full sequence 의 TPX 와 동일한 염증억제 효과가 있는 가장 작은 TPX 인 것을 밝힐 수 있었다. 결과적으로 이 논문은 간흡충 분비배설항원과 작은 T44 TPX 가 LPS 의 조절역할을 함으로써 염증을 억제한다는 것을 명시한다. 작은 TPX T44 는 알러지 또는 자가면역 질환과 같은 면역 질환의 효과적인 면역억제 치료제로써의 개발 가능성을 내포하고 있다.

주요어 : 간흡충, 항산화효소, 면역 회피 기전, 대식세포, 사이토카인

학 번 : 2010 – 31160